

Review

Antioxidant Determination with the Use of Carbon-Based Electrodes

Aurelia Magdalena Pisoschi ^{1,*} , Aneta Pop ¹, Florin Iordache ¹ , Loredana Stanca ¹, Liviu Bilteanu ^{1,2} and Andreea Iren Serban ^{1,3}

¹ Faculty of Veterinary Medicine, University of Agronomic Sciences and Veterinary Medicine of Bucharest, 050097 Bucharest, Romania; aneta_pop_ro@yahoo.com (A.P.); floriniordache84@yahoo.com (F.I.); lory_stanca@yahoo.com (L.S.); bilteanu.md@gmail.com (L.B.); irensro@yahoo.com (A.I.S.)

² Molecular Nanotechnology Laboratory, National Institute for Research and Development in Microtechnologies, 077190 Bucharest, Romania

³ Department of Biochemistry and Molecular Biology, Faculty of Biology, University of Bucharest, 050095 Bucharest, Romania

* Correspondence: aureliamagdalenapisochi@yahoo.ro

Abstract: Antioxidants are compounds that prevent or delay the oxidation process, acting at a much smaller concentration, in comparison to that of the preserved substrate. Primary antioxidants act as scavenging or chain breaking antioxidants, delaying initiation or interrupting propagation step. Secondary antioxidants quench singlet oxygen, decompose peroxides in non-radical species, chelate prooxidative metal ions, inhibit oxidative enzymes. Based on antioxidants' reactivity, four lines of defense have been described: Preventative antioxidants, radical scavengers, repair antioxidants, and antioxidants relying on adaptation mechanisms. Carbon-based electrodes are largely employed in electroanalysis given their special features, that encompass large surface area, high electroconductivity, chemical stability, nanostructuring possibilities, facility of manufacturing at low cost, and easiness of surface modification. Largely employed methods encompass voltammetry, amperometry, biamperometry and potentiometry. Determination of key endogenous and exogenous individual antioxidants, as well as of antioxidant activity and its main contributors relied on unmodified or modified carbon electrodes, whose analytical parameters are detailed. Recent advances based on modifications with carbon-nanotubes or the use of hybrid nanocomposite materials are described. Large effective surface area, increased mass transport, electrocatalytical effects, improved sensitivity, and low detection limits in the nanomolar range were reported, with applications validated in complex media such as foodstuffs and biological samples.

Keywords: antioxidants; carbonaceous electrodes; electroanalysis; voltammetry; amperometry; potentiometry



Citation: Pisoschi, A.M.; Pop, A.; Iordache, F.; Stanca, L.; Bilteanu, L.; Serban, A.I. Antioxidant Determination with the Use of Carbon-Based Electrodes. *Chemosensors* **2021**, *9*, 72. <https://doi.org/10.3390/chemosensors9040072>

Academic Editor: Khiena Z. Brainina

Received: 13 February 2021

Accepted: 29 March 2021

Published: 1 April 2021

Publisher's Note: MDPI stays neutral with regard to jurisdictional claims in published maps and institutional affiliations.



Copyright: © 2021 by the authors. Licensee MDPI, Basel, Switzerland. This article is an open access article distributed under the terms and conditions of the Creative Commons Attribution (CC BY) license (<https://creativecommons.org/licenses/by/4.0/>).

1. Antioxidants—General Aspects and Main Determination Techniques

1.1. Defining, Classifying and Describing Modes of Action Antioxidants

Antioxidants are chemical species that prevent or delay oxidation processes. They originate from various sources and hamper lipid peroxidation following different mechanisms of intervention, acting at a much smaller concentration, in comparison to that of the preserved compound [1–5].

Primary antioxidants act as scavenging or chain breaking antioxidants, delaying initiation or disrupting propagation. Secondary antioxidants quench singlet oxygen, decompose peroxides in non-radical species, chelate prooxidative metal ions, inhibit oxidative enzymes or absorb UV radiation. It has been confirmed that they can exploit the above-described mechanisms to stabilize/regenerate primary antioxidants [1].

Considering antioxidants' reactivity, four lines of defense have been described. Antioxidants belonging to the first line of defense withhold radical species generation. The second

line of defense includes mainly radical scavenging antioxidants. The third line of defense intervenes after the free radical-caused insults, being composed of repair antioxidants. Adaptation mechanisms underlie the mode of action of the fourth line of defense: Signals required for free radical generation are exploited, thus such antioxidants can disrupt free radical occurrence or reactions implying radical species intervention [6,7].

Superoxide dismutase, catalase, glutathione peroxidase, metal-binding proteins like lactoferrin, ferritin, caeruloplasmin, glutathione, uric acid, alpha-lipoic acid, ubiquinones, bilirubin, and melatonin are well-recognized endogenous antioxidants. Tocopherols, phenolics, vitamin C, and carotenoids are exogenous antioxidants found in food and /or dietary supplements, slowing up the use of endogenous antioxidants, so the cell's own antioxidant profile can remain unaltered [1,8].

Synthetic antioxidants such gallic acid esters, synergistic butylated hydroxyanisole and butylated hydroxytoluene are added to foodstuffs to prevent rancidity. Another antioxidant classification takes account on the solubility: Hydrophilic (ascorbic acid, glutathione, uric acid, flavonoids) and lipophilic (carotenoids, tocopherols, ascorbyl palmitate, or stearate) antioxidants [1].

With respect to the mechanism involved in free radical inactivation, antioxidant can follow either hydrogen atom transfer, or single electron transfer. Hydrogen atom transfer is swift and is not dependent on pH or nature of solvent, but proved sensitive to the presence of other reductant species. The behavior of an antioxidant molecule can also encompass single electron transfer [9,10]. Considering the analytical methods developed, hydrogen atom transfer underlies Oxygen Radical Absorbance Capacity (ORAC), Total Radical Trapping Antioxidant Potential (TRAP) and chemiluminescence, whereas single electron transfer underlies Ferric reducing ability of plasma (FRAP), and Cupric Reducing Antioxidant Capacity (CUPRAC) [2,10]. 2,2-diphenyl-1-picrylhydrazyl (DPPH) and Trolox Equivalent Antioxidant Capacity (TEAC) can exploit both mechanisms [10,11].

Antioxidants can hamper the deleterious effects of free radicals in the human body, as well as the oxidative decay of food components [1–3,12–14]. Although both terms have been employed in papers approaching antioxidant assay, distinction has been drawn between antioxidant activity and antioxidant capacity. The antioxidant capacity reflects the conversion of the reactive oxygenated species that is scavenged. This illustrates the scavenging ability, and can be expressed as the amount, as moles, of the scavenged free radical by antioxidants [15,16], present in an analyzed sample, for instance a plant extract [17]. The term “antioxidant activity” is prevalent in electrochemical approaches, that directly provide informations about analyte concentration. Hence, “antioxidant activity” is linked to a thermodynamic significance, as it can be correlated to the total active or effective concentration of antioxidants, or oxidants in a sample. It can be expressed as units of standard antioxidant, for instance milligrams, mmoles or μ moles Trolox equivalents or other reference antioxidant (ascorbic acid, gallic acid, quercetin, catechin, rutin), per amount (grams, kilograms, liters, etc.) of sample. “Antioxidant power” and “antioxidant ability” are less used, and they do not have a precise interpretation [18].

1.2. Analytical Methods Applied to Antioxidant Determination

1.2.1. General Overview of Methods

Antioxidant assay can rely on a plethora of methods, based on electrochemical, spectrometrical or chromatographic detection [4,19,20]. A synoptic overview of the principles underlying the main analytical techniques and detection systems applied to antioxidant assay is presented in Table 1 [21–62].

Table 1. The main analytical methods applied to antioxidant assay [21–62].

Total Antioxidant Capacity or Its Main Contributors' Assay	Method's Principle	Detection of the End-Product	Ref.
Spectrometry			
DPPH	Antioxidants react with an organic radical	Colorimetric	[21,22]
ABTS	Antioxidants react with an organic cation radical	Colorimetric	[23,24]
FRAP	Antioxidants react with ferric-tripyridyltriazine complex	Colorimetric	[25,26]
PFRAP	Potassium ferricyanide is reduced by antioxidants to potassium ferrocyanide, that reacts with Fe ³⁺ yielding ferric ferrocyanide	Colorimetric	[27,28]
CUPRAC	Antioxidants reduce Cu (II) complex to a Cu (I) complex	Colorimetric	[29,30]
Thiobarbituric Acid Reactive Species (TBARS) Assay	The generation of malonyl dialdehyde can be detected after its reaction with thiobarbituric acid, yielding a pink chromogen	Colorimetric assay of malonyl dialdehyde-thiobarbituric acid adduct	[31,32]
Folin-Ciocalteu	Phenolics react with a mixture of phosphomolybdate/phosphotungstate in the presence of sodium carbonate 20%.	Absorbance of the blue molybdenum-tungsten complex resulted is measured, versus gallic acid as reference antioxidant	[33,34]
ORAC	Peroxy radicals, induced by AAPH (2,2'-azobis-2-amidino-propane) decomposition are reduced by antioxidants	Loss of fluorescence indicated by fluorescein	[35,36]
HORAC	Co(II)-based Fenton systems result in OH radicals generation, followed by quenching by antioxidants	Loss of fluorescence indicated by fluorescein	[37,38]
TRAP	Luminol-derived radicals, formed by AAPH decomposition, are scavenged by antioxidants	Quenching of chemiluminescence	[39,40]
Fluorimetry	Emission of electromagnetic radiation (generally in the visible range) that follows an absorption process (generally in the UV domain)	Recording of excitation/emission spectra of fluorescent reagent	[41,42]
Electrochemical Techniques			
Potentiometry	Antioxidants interact with the oxidized form of a redox couple, changing the ratio between the oxidized form and the reduced form concentration	The analytical signal recorded is the potential shift of the mediator system, resulting from interaction with antioxidants	[43,44]

Table 1. Cont.

Total Antioxidant Capacity or Its Main Contributors' Assay	Method's Principle	Detection of the End-Product	Ref.
Cyclic voltammetry (CV)	Linear variation of the potential of a working electrode following a triangular waveform, and recording of current intensity	The intensity value corresponding the cathodic/anodic peak is measured	[45,46]
Differential pulse voltammetry (DPV)	Voltage pulses are superimposed on the potential scan, that is varied linearly or staircase-wise	First intensity value is sampled before applying the pulse, and the second towards the end of the pulse	[47,48]
Square-wave voltammetry (SWV)	A square wave is superimposed on a potential staircase sweep variation	Current intensity recorded at the end of each potential change	[49,50]
Polarography	Determination of the antioxidant potential of radical scavengers relied on the anodic oxidation of dropping mercury electrode	Diminution of the anodic limiting current of the hydroxoperhydroxomercury(II) complex, $[\text{Hg}(\text{O}_2\text{H})(\text{OH})]$, generated in H_2O_2 solution at alkaline pH, at the potential of Hg oxidation	[51,52]
Amperometry	Measurement of the current intensity at a fixed potential value of the working electrode, with respect to a reference one	The intensity of the current, occurring as result of oxidation/reduction of the analyte at constant potential, is measured	[53,54]
Biamperometry	Reaction of the antioxidant with the oxidized form of a reversible indicator redox couple	The current flowing between two identical working electrodes is measured, at a small potential difference; the measuring solution contains the antioxidant(s) in the presence of a reversible redox couple	[55,56]
Chromatography			
Gas chromatography (GC)	The compounds to be separated and quantified are differentially distributed between a liquid stationary phase and a gaseous mobile phase	Detection based on thermal conductivity or flame ionisation	[57,58]

Table 1. Cont.

Total Antioxidant Capacity or Its Main Contributors' Assay	Method's Principle	Detection of the End-Product	Ref.
High performance liquid chromatography (HPLC)	The compounds to be separated suffer different repartition between a solid stationary phase and a liquid mobile phase with various polarities, at high values of pressure of the mobile phase and flow rate	Diode array (UV-VIS), mass spectrometry, fluorescence, or electrochemical detection	[59,60]
Thin layer chromatography (TLC)	Compound separation relies on the repartition between a solid stationary phase (silica gel, alumina) and a liquid mobile phase (methyl acetate/formic acid, ethanol/hexane, or methanol/chloroform/ hexane)	UV-VIS visualization, fluorescence or phosphorescence detection	[61,62]

The advantages and shortcomings of the methods applied in antioxidant assay have been described by Sadeer et al. [20]. Photometric techniques such as DPPH, ABTS are rapid, simple, and provide reproducible results, whereas TBARS assay is characterized by not so good sensibility and specificity [20]. Chromatographic techniques offer accurate and reproducible results, but are often laborious, time-consuming, and require specialized equipment and skilled personnel. Electroanalytical techniques benefit from the rapidity and sensitivity of the electrochemical detection, with specificity improvable by the use of mediators and enzymes in modified electrodes.

1.2.2. Electrochemical Techniques

This sub-section provides a characterization of electroanalytical techniques applied to individual antioxidant content and antioxidant activity determination. Voltammetric and amperometric/biamperometric methods are the most broadly used.

These techniques are able to provide direct assay of the total antioxidant activity, even in the absence of reactive species. Voltammetric and amperometric techniques, including integration in flow injection analysis set-up and microfluidic chip configurations coupled with amperometric detection, relate oxidation potential to antioxidant activity [63,64]. Developing enzyme electrodes by biocatalyst incorporation enables viable assay of the total antioxidant profile or total phenolics, with quantitation in food and beverages, biological samples, pharmaceuticals [63].

Cyclic voltammetry (CV) as potentiodynamic technique involves linear variation applied to the working electrode's potential, in a triangular waveform, and the recording of the current intensity. The anodic oxidation and cathodic reduction potentials (E_a and E_c) furnish qualitative informations, whereas the intensities of the anodic and cathodic peaks (I_a , I_c) are related the analyte's amount. For reversible systems, the values of the intensities of the cathodic and anodic peaks are equal. For irreversible systems, the presence of one peak can be noticed on the voltammogram. Cyclic voltammetry has proved its analytical viability for the quantitation of low molecular weight antioxidant capacity of plant extracts, tissue homogenates and blood plasma. The oxidation potential and half-wave potential are linked to the nature of the antioxidant analyte(s); the intensity of the current measured for the anodic peak and the area of the anodic wave underlie quantitative assay [45].

Differential pulse voltammetry (DPV) implies one measurement before applying the potential pulse, and a second towards the end of the pulse period. Sampling the current just before the potential is changed, lowers the effect of the charging current and enhances

faradaic current. In differential techniques, the advantage consists in measuring the $\Delta i/\Delta E$ value, where Δi is the difference between the current intensity values, taken just before pulse application, and at the end of the pulse period. Another consequence of double intensity measurement is the presence of the analytical signals in the form of sharp peaks, with improved resolution and sensitivity [53].

Square-wave voltammetry (SWV): A square-wave is superimposed on the potential staircase variation, whereas the current is recorded at the end of each potential change, minimizing charging current, just as in differential pulse technique. Square-wave voltammetry facilitates data acquisition with high sensitivity and minimization of background signals. The fast potential scan enables repetitive measurements, with signals acquired at optimized signal-to-noise ratio. The technique benefits from high contribution of the faradaic current, increased resolution and sensitivity [53].

Staircase voltammetry is a derivative of the linear scan technique less applied in antioxidant assay, for which the potential sweep is a succession of stair steps. The current intensity is measured at the end of each potential change, just before the following step, so contribution of capacitive current is lowered.

Chronoamperometry relies on applying single or double potential steps, and the current resulting from faradaic processes that occur at the electrode is measured as a function of time. As in the case of other pulsed techniques, generated charging currents exponentially decline with time. The Faradaic current due to electron transfer diminishes as revealed by Cottrell equation, that illustrates the inverse dependence of the recorded intensity response, on the square root of time (seconds), under diffusion-controlled conditions. By integrating current intensity over longer periods of time, chronoamperometry improves signal to noise ratio versus other amperometric methods.

Chronocoulometry relies on analogous principles, but it records the variation of charge with time, instead of the current–time dependence. Nevertheless, in chronocoulometry, a signal increase in time is monitored instead of a decrease; signal integration diminishes noise, resulting in a smooth hyperbolic curve; the contributions of absorbed or double-layer charging species become readily noticeable.

Polarography: Polarography is a particular variant of linear sweep voltammetry, that makes use of mercury drop electrode [52]. As a technique with linear potential scan, it is controlled by mass transport, and the recorded polarograms (the current versus potential dependences) have a characteristic sigmoidal shape. The current oscillations noticed on the polarogram are assigned to the mercury drops that fall from the capillary. The limiting current is a diffusion one, as diffusion is the main contributor to the flux of electroactive compounds towards the electrode. The method may suffer from a significant capacitive current contribution, due to the continuous current measurement. Recently, a Clark's standard Pt electrode was employed for antioxidant activity assay, relying of the measurement of the rate of oxygen intake of a microsomal suspension [51].

The amperometric method: Amperometry involves the measurement of the intensity of the current generated by the oxidation/reduction of an electroactive analyte. During this type of electrochemical assay, the value of the potential is maintained at a fixed value with respect to a reference electrode [65]. The current measured at constant potential due to the oxidation/reduction of the electroactive analyte can be directly correlated to the concentration of the latter. The performances of this technique depend on the working potential. Lowering of the latter, with improvable sensitivity and selectivity, is possible by the use of mediators or enzyme incorporation [53].

The biamperometric method: Biamperometry relies on the measurement of the current flowing between two identical working electrodes, at a small potential difference. Biamperometric selectivity is dependent on the specificity of the reaction between the analyte and the oxidized/reduced form of the redox pair and the analyte. A redox pair largely used in biamperometric studies is DPPH•/DPPH. The recorded analytical signal is proportional to the residual concentration of DPPH•, after its reaction with the antioxidant. Other redox couples used in biamperometric antioxidant capacity assay are ABTS⁺/ABTS, Fe³⁺/Fe²⁺,

$\text{Fe}(\text{CN})_6^{3-}/\text{Fe}(\text{CN})_6^{4-}$, $\text{Ce}^{4+}/\text{Ce}^{3+}$, $\text{VO}_3^-/\text{VO}^{2+}$, and I_2/I^- [56,66,67]. The assay of total antioxidant capacity has been applied to the analysis of alcoholic beverages [56] and juices [68].

Potentiometry: Potentiometric measurements logarithmically correlate the electrochemical cell's potential to the analyte concentration. Lowered potentials signify enhanced electron-donating abilities and, consequently, increased antioxidant potentials. Potentiometry does not need current or potential modulation as in voltammetry/amperometry [53]. It relies on the potential variation that results from a change in the ratio oxidized form/reduced form of an indicating redox species. With the increase of the antioxidant level, the concentration of the reduced form of the indicator increases, and the subsequent potential change is recorded [69]. Possible drawbacks in ion selective potentiometry can encompass deviations from Nernst's equation, caused by changes in ion activity or temperature.

1.2.3. Biosensor Methods

Biosensors have been applied to the assay of compounds endowed with reductive/antioxidant properties [70,71]. Oxido-reductases are often encountered in biosensor applications, due to the confirmed enhanced electron transfer ability. Biocatalysts act at low concentrations when compared to those of the target analytes (substrates) and do not always require the presence of cofactors. Laser-derived graphene sensors based on nanomaterials and conducting polymers were applied in environmental monitoring, food safety assay, and clinical diagnosis [72]. The use of multienzyme systems in electrochemical biosensors enables detection of a broad spectrum of compounds, as well as the improvement of electrochemical biosensor's analytical parameters, selectivity and sensitivity [73].

A series of review papers and books refer to antioxidant and antioxidant capacity assay by the use of biosensors [74–79]. Applications of biosensors for assessing antioxidant potential are based on monitoring superoxide anion radical ($\text{O}_2^{\bullet-}$), nitric oxide (NO), glutathione, uric acid, phenolics, or ascorbic acid [80]. A carbon paste biosensor developed by DNA incorporation relied on the partial damage of the DNA layer present on the electrode surface by $\text{OH}\bullet$ radicals, produced in a Fenton system. The electro-oxidation of the intact-remaining adenine nucleobases, generated an oxidation product able to catalyse NADH oxidation. Sample antioxidants scavenged $\text{OH}\bullet$, so more adenine molecules were left unoxidized, resulting in an increase of the catalytic current given by NADH oxidation, quantified in differential pulse voltammetry. Ascorbic acid served as model antioxidant, enabling quantitation of levels as low as 50 nM ascorbic acid in aqueous media [81].

Amperometric biosensors applied in the assessment of phenolics, major contributors to the antioxidant capacity of plants, incorporated laccase, tyrosinase, or peroxidase [82–85]. Phenolic compounds could be quantitated by enzyme sensors developed by immobilizing polyphenol oxidase (PPO) into conducting copolymers obtained by co-electropolymerization of pyrrole with thiophene-capped polytetrahydrofuran [84]. Phenolic compounds are also determined using biosensors based on oxidases such as tyrosinase and laccase [86].

The principles of developing and particular applications of carbon-based sensors will be discussed in the next sections, given the increasing need for high performance analytical tools in the field of antioxidant assay, linked to food quality and health status monitoring.

2. Carbon Electrodes—General Overview

Carbon electrodes are largely employed in electroanalysis due to their special features, that encompass large surface area, tunable porosity, high electroconductivity, chemical stability, temperature resistance, nanostructuring possibilities, facility of manufacturing at low cost, and easiness of surface modification. The carbonaceous electrodes were classified as carbon paste, glassy carbon, fullerenes, graphite, diamond, and screen-printed electrodes [87].

Carbon Paste Electrodes: Carbon paste electrodes are synthesized from graphite powder and various water-immiscible nonelectrolytic organic pasting liquids, such as mineral (paraffin) oil, [88,89]. Most often high purity mineral oil (Nujol) is employed, nevertheless quasi-solid binders such as silicone grease or polypropylene could replace commonly used pasting liquids, but the developed structure has much higher density and becomes less easy to handle [90]. The advantages of carbon paste electrodes are facility of including modifiers (for developing novel, redox-mediated sensors), very low ohmic resistance, minimized toxicity of this environmentally compatible material, reduced background current, individual polarizability [87]. Obtaining carbon paste electrodes can also be rely on alternative carbon-based materials, replacing graphite powder with glassy carbon powder, carbon nanotubes, porous carbon foam, acetylene black [90].

Glassy Carbon Electrodes: Glassy carbon, also called vitreous carbon is a type of nongraphitizing, solid, three-dimensional carbon material, broadly used in electro-assay. It is obtained at temperatures above 2000 °C, to decompose pyrolysis intermediates that generally exhibit a scarce thermal conductivity [91]. The surface of glassy carbon electrodes can be modified with functional nanomaterials (metals, alloys, or metal oxides) [92,93]. Glassy carbon and glassy carbon-based electrodes provide excellent electroconductivity, mechanical resistance, broad potential range, and gas impermeability [87]. They have large potential window and chemical stability, prove better resistance to solvents than metal electrodes, been confirmed for their viability at the assay of organic compounds. Bare glassy carbon electrodes are characterized by facility of use, being mechanically cleaned by mere polishing on alumina slurry, procedure that can be followed by sonication in aqueous medium. Nevertheless, residual alumina particles on the electrode surface can affect the recorded electrochemical profile of electroactive analytes endowed with reductive (antioxidant) potential, such as phenolics [94].

Glassy carbon modification with alumina particles aimed at improving sensitivity in the case of dopamine [95]. The application of alumina-modified glassy carbon electrode promotes sensitivity, detectability and selectivity in the case of nitroaromatic compounds. Enhancement of dissolved oxygen electrochemical reduction in the presence of alumina was also reported [96]. Employing alumina suspensions for modifying glassy carbon electrodes by abrasive polishing, resulted in successful electro-assay of various phenolics. Modification of glassy carbon electrodes with α -alumina resulted in improved electrochemical response in comparison with θ and γ -alumina, and it was confirmed that alumina structure, and not the particle size or surface area, can exert notable effects [97].

Glassy carbon modification with alumina enhanced the voltammetric current response of gallic acid, caffeic acid, chlorogenic acid, catechin, quercetin, and rutin. By applying this simple procedure of electrode modification, lowered DPV relative standard deviation (RSD < 3%, n = 5) for repetitive assays and high inter-electrode precision (RSD < 4%, n = 3) were reported. Nevertheless, when use of unmodified glassy carbon electrodes is chosen, the application of the sonication step to remove all residual alumina is compulsory, as alumina remaining on the electrode surface can significantly affect the voltammetric profile of sample antioxidants [98].

The use of other metal oxides for modification, may also provide performance improvement in the electrochemical determination of antioxidant species. Modification with metal (gold, silver and platinum) or metal oxide nanoparticles imparts distinctive size-dependent electrochemical features. The sol-gel chemistry served for developing silica-modified electrodes, exploiting silica adsorption properties [98,99].

Carbon nanomaterials were divided into: Zero-dimensional fullerenes [100], one dimensional carbon nanotubes [101], two-dimensional graphene [102], and the three-dimensional porous carbons [103]. Porous carbon materials are fabricated using precursors named template composite materials which are synthesized, with subsequent carbonization and template removal [104]. Nevertheless, such a technique is laborious and necessitates a series of synthetic steps, the first stage of template injection, the etching process and

the long solidification time [105], which may restrict mass applications of porous carbon materials [106].

Fullerene Electrodes: Fullerenes represent a class of carbon compounds in which carbon atoms form closed cage or cylinder-shaped structures. In the first case the compound is called Buckminsterfullerene (C₆₀, named after the American architect R. Buckminster Fuller, whose geodesic dome was constructed relying on the same structural principles), and in the second case, the obtained structure is called carbon-nanotube [107–109]. Single-walled and multi-walled carbon nanotubes are widely employed in electrode modification, being biocompatible, having large surface area to volume ratio, enhanced electro-conductivity, chemical and mechanical resistance.

In the structure of graphene, atoms constitute a single layer and are placed in a two-dimensional honeycomb lattice. Each atom uses sp² hybridized orbitals to connect by sigma bonds to its three nearest neighbors, and contributes with one electron (belonging to the p unhybridized orbital) to the conduction band that is common for the whole sheet. This type of bond is also encountered in carbon nanotubes, fullerenes and glassy carbon. Graphene oxide nanoparticles, alongside metal oxide nanoparticles are largely used in electrode modification, aiming at antioxidant determination. The oxygenated groups can lead to improvement in the electrochemical responses and mechanical properties. The polarity of these groups present at the surface of graphene oxide results in high dispersibility in polar solvents, enabling applications in biosensing systems.

Graphite Electrodes: Graphite is an allotropic form of carbon, where sp²-hybridized atoms form planes of hexagonal bonds. Graphite is a stable crystalline form of carbon, which can be employed as such, or in the form of composites [110–113]. Electrodes are inexpensive, commercially available and easy to modify, so they benefit from selectivity enhancement through various modifications, renewable surfaces and hazard-free polishing [114]. The high delocalization degree of pi electrons and the weak van der Waals interactions between the layers, result in good electro-conductivity.

Diamond Electrodes: Diamond is an allotrope form of carbon with insulating properties, very good mechanical resistance, the hardness being due to the bonds established between sp³ carbon atoms. Diamond is a non-easily accessible material, whose preparation require high temperatures and pressures [115]. By doping diamond with boron in different proportions, conductive, superconducting or semiconductor materials can be synthesized. These electrodes are chemically inert and are endowed with excellent electrical features. High boron-doped (10³–10⁴ ppm) diamond has metal-like conductivity and can be applied as electrode material [116]. Boron-doped polycrystalline diamond exhibits a rougher morphology, a higher sp³ content, a broader water potential window, and a lower background current [117].

Screen-Printed Electrodes: Such electrodes are developed by printing inks on ceramic or plastic surfaces. The inks, depending on the composition (carbon, gold, platinum) will determine the characteristics of screen-printed electrodes, that can be part of a three electrode set-up in a measuring cell. Depending on the target analyte, the ink can be modified by incorporation of metal powders, redox complexes or biocatalysts, to promote electron transfer [118–120].

Glassy carbon, vitreous carbon, carbon nanotubes, fullerenes, screen-printed, graphite, and diamond electrodes are considered homogenous carbon electrodes, whereas carbon paste and modified carbon pastes are heterogeneous carbon electrodes.

In a recent study, a detailed description of advantages and shortcomings of several broadly employed types of carbon-based electrodes is provided [121].

Carbon paste electrodes offer an analytical response on wide potential ranges, with small background current, reduced ohmic resistance, and facility of tuning pretreatment methods and surface modification. These materials do not harm the environment and operate at low cost. Nevertheless, they were characterized as not stable for functioning in flow systems, are not compatible with organic solvents, and often require recalibration. When using organic compounds as binders, the use of such sensors results in irreversibility

of recorded voltammograms, and the surface roughness can influence reproducibility of the response.

Glassy carbon electrodes exhibit high mechanical resistance and excellent electroconductivity. They are characterized by chemical inertness and function on large potential domains, over wide pH ranges, from strongly acidic to alkaline environment. Their large size and difficulty to manufacture at large scale may constitute inconveniences. The electron transfer occurs slower than at electrodes based on noble metals.

Carbon fiber microdisk electrodes are easy to use due to their small diameter and benefit from high speed of electron transfer. They give a rapid analytical response and exhibit high sensitivity for small concentration changes. Being compatible with biological media and non-toxic to cells, can be applied successfully to in vivo determinations. Nevertheless, they may not exhibit resistance to the mechanical force or to the high temperatures applied during the step of capillary pulling. Low selectivity and the possibility to break glass insulation during in vivo measurements are other disadvantages.

Basal plane pyrolytic graphite electrodes are characterized by high speed electrode reaction kinetics, with lowered background signal. Shortcomings may be the irreversible behavior and the large dimensions.

Screen-printed carbon electrodes are easy to employ, due to portability and facility to apply modifications. A broad series of geometries can be obtained, and the determinations can be performed with the possibility to eliminate surface fouling, and low cost. Nevertheless, the incorporated binders may alter the shape of voltammograms. Fouling of the electrode surface may be caused by products of redox reactions. Other shortcomings may be the rough surface and the slow reaction kinetics. The organic solvents present in the buffer may dissolve the ink, diminishing sensitivity.

Given the confirmed advantages of boron-doped diamond (excellent electroconductivity, mechanical resistance), the behavior of this type of electrode has been investigated in cyclic voltammetry of gallic acid. At low potentials, when the electrolytes are stable, deactivation of boron-doped diamond has been reported. It was found that gallic acid electro-oxidation generated the occurrence of a polymeric film on the anodic surface, causing boron-doped diamond deactivation [122].

3. Determination of Individual Antioxidants with Carbon-Based Electrodes

The determination of individual key antioxidants relied on a series of unmodified or modified carbon-based electrodes. An overview of the analytical parameters and applications on real samples, at the assay of some individual antioxidants, using carbonaceous working electrodes is presented in Table 2 [123–167].

Table 2. Electroanalytical techniques applied to the assay of key individual antioxidants [123–167].

No	Antioxidant	Analytical Method	Carbon-Based Working Electrode	Analytical Characteristics	Ref.
1.	Ascorbic acid (AA)	Cyclic voltammetry; Differential pulse voltammetry;	-carbon paste electrode;	-linear range 0.07–20 mM -supporting electrolyte: KCl 0.1 M; -RSD 2.35% in DPV and 2.29% in CV; -LOD 0.018 mM (CV) and 0.02 mM (DPV), calculated as 3× square mean error (for 10 determinations of the blank)/the slope of the calibration graph; -LOQ 0.062 mM (CV) and 0.068 mM (DPV), calculated as 10× square mean error (for 10 determinations of the blank)/the slope of the calibration graph; -analysis of commercial and home-made fruit juices; -oxidation peaks at 470 mV in DPV and at 510 mV in CV (vs SCE);	[123]

Table 2. Cont.

No	Antioxidant	Analytical Method	Carbon-Based Working Electrode	Analytical Characteristics	Ref.
2.	Ascorbic acid	Differential pulse voltammetry;	-screen-printed carbon electrode;	-determinations performed in phosphate buffer solutions (pH: 5.8, 7.0 and 7.4); -oxidation peak potentials increasing with concentration, noticed between -0.02 V and 0.11 V (vs. Ag/AgCl); -linear range of 1 to 4 μM (pH 5.8) and 2 – 10 μM (pH 7.0), as present in calibration curve; -assay of injectable vitamin C solutions;	[124]
3.	Ascorbic acid Dopamine Paracetamol	Cyclic voltammetry; Differential pulse voltammetry; Chronoamperometry;	-platinum nanoparticles-decorated graphene nanocomposite electrode, compared with graphene-modified glassy carbon electrode and bare glassy carbon electrode;	-supporting electrolyte: KCl 0.1 M; -linear range 300 μM to 20.89 mM (for AA in CV); -LOD of 300 μM (for AA in CV); -AA exhibited two linear DPV ranges, 300 μM to 7.36 mM and 8.12 to 39.87 mM; -LOD 5 μM (AA in DPV); -linear range from 420 μM to 29.26 mM for ascorbic acid in chronoamperometry, at 0.0 V vs. Ag/AgCl used as reference;	[125]
4.	Ascorbic acid	Cyclic voltammetry; Chronoamperometry; Linear sweep voltammetry (LSV);	-carbon veil electrode modified with phytosynthesized gold nanoparticles;	-LSVs recorded from 0.0 V to $+0.8$ V, vs. Ag/AgCl, at a scan rate of 0.05 Vs^{-1} ; -supporting electrolyte: Phosphate buffer pH 5.0 to 8.0 ; -modification with gold nanoparticles shifted the cyclic voltammetric potential of AA oxidation with more than 0.4 V towards less positive values; -linear response to AA 1 μM – 5.75 mM in anodic voltammetry; -LOD 0.05 μM and LOQ 0.15 μM (CV); -most increased oxidation current of AA obtained in pH 6.0 phosphate buffer solution; -analysis of fruit juices;	[126]
5.	Ascorbic acid Uric acid Cholesterol	Cyclic voltammetry; Square-wave voltammetry;	-carbon paste electrode modified with copper oxide-decorated reduced graphene;	-supporting electrolyte: Phosphate buffer pH 7.4 ; -scan rates (CV) of 10 , 25 , 50 , 100 , 150 , 200 , 250 , 300 , 500 mV s^{-1} , for 500.0 μM cholesterol, using Ag/AgCl as reference; -linear response to AA 0.04 – 240.0 μM , with a LOD of 9 nM (SWV); -linear response to uric acid 0.04 – 400 μM , with a LOD of 8 nM (SWV); -linear response to cholesterol 0.03 – 300 μM , with a LOD of 9 nM (SWV); -differences between peak potentials (SWV) as follows: 430 mV (between cholesterol and ascorbic acid), 270 mV (between ascorbic acid and uric acid) and 700 mV (between cholesterol and uric acid);	[127]

Table 2. Cont.

No	Antioxidant	Analytical Method	Carbon-Based Working Electrode	Analytical Characteristics	Ref.
6.	Delphinidin, Cyanidin, Pelargonidin, Kuromanin, Callistephin	Cyclic voltammetry; Differential pulse voltammetry;	-glassy carbon electrode;	-supporting electrolyte: Methanol containing 0.1 mol L ⁻¹ lithium perchlorate or 0.1 mmol L ⁻¹ Britton-Robinson buffer; -pulse amplitude of 50 mV, pulse width of 70 ms, and scan rate of 10 mV s ⁻¹ (DPV); -cyclic voltammetric scan rates ranging from 25 mV s ⁻¹ to 500 mV s ⁻¹ ; -oxidation peak potentials comprised between 519 and 1115 mV vs Ag/AgCl (CV); -the larger the number of hydroxyl groups in the B ring, the lower the oxidation potential; -sugar moieties result in displacement of peak potentials to more positive values;	[128]
7.	Oenin chloride; Malvin chloride; Kuromanin chloride; Cyanin chloride; Myrtillin chloride; Petunidin chloride;	Cyclic voltammetry; Differential pulse voltammetry; Square-wave voltammetry;	-glassy carbon electrode;	-supporting electrolytes: Acetic acid/acetate buffer pH 3.5 and 4.5, as well as phosphate buffer pH = 7.0; -voltammetric scans in the potential range of 0 to +1.4 V vs. Ag/AgCl; -differential pulse voltammetric pulse amplitude 50 mV, pulse width 70 ms and scan rate 5 mVs. ⁻¹ ; -square-wave voltammetric frequency 13, 25 and 50 Hz; amplitude 50 mV and potential increment 2 mV; -first cyclic voltammetric oxidation peak appears at 0.3 V for kuromanin chloride as well as for cyanin chloride, with a corresponding cathodic peak at 0.23 V in phosphate buffer pH = 7.0; -kuromanin chloride showed a DPV oxidation peak potential at 0.49 V and peonidin-3-O-glucoside at 0.39 V, in 0.2 M acetate buffer, pH 3.5;	[129]
8.	Delphinidin-3-O-glucoside; Malvidin-3-O-glucoside-catechin; Peonidin-3-O-glucoside-4-vinylphenol, etc.;	Cyclic voltammetry; Differential pulse voltammetry;	-glassy carbon electrode;	-supporting electrolytes: Acetate-acetic acid buffer pH 3.6, and acetate-acetic acid buffer pH 3.6, containing 12% ethanol; -cyclic voltammograms obtained in the range of 0 to +0.8 mV, at a scan rate of 100 mV/s; -differential pulse voltammetric measurements performed with a pulse amplitude of 50 mV and a pulse width of 50 ms; -20-fold diluted wine presented DPV peak potentials of 443 mV and 666 mV vs Ag/AgCl, similar to those of wine extract, and to those of malvidin-3-O-glucoside (53.6% of the total anthocyanin content in grape extract); -20-fold diluted wine presented one oxidation peak, at 491 mV in CV; -ascorbic acid (0.05–0.1 mg/mL) used as reference, presented an oxidation peak at 270 mV in DPV;	[130]

Table 2. Cont.

No	Antioxidant	Analytical Method	Carbon-Based Working Electrode	Analytical Characteristics	Ref.
9.	Malvidin-3-glucoside, Catechin, Epicatechin, Gallic acid, Hydroxycinnamic acids, etc.	Square-wave voltammetry;	-glassy carbon electrode;	-disposable unmodified screen-printed carbon electrodes; -screen-printed carbon electrodes modified with single- and multi-walled carbon nanotubes; -determinations performed in a model wine solution: 12% (v/v) ethanol, containing 33 mM l-tartaric acid, at pH 3.6; -Ag/AgCl as reference electrode; -characterization of red wine polyphenols; -at the single-walled carbon nanotubes-modified screen-printed carbon electrode, first peak obtained between 138 mV (gallic acid) and 340 mV (malvidin-3-O-glucoside); -at the multi-walled carbon nanotubes-modified screen-printed carbon electrode, first peak obtained between 120 mV (gallic acid) and 370 mV (malvidin-3-O-glucoside);	[131]
10.	β -carotene	Cyclic voltammetry;	-glassy carbon electrode;	-supporting electrolyte: 0.1 M LiClO ₄ in ethanol containing 10% CH ₂ Cl ₂ ; -potential scan rate of 100 mV s ⁻¹ ; -potential range from 0 to 1500 mV; -beta-carotene irreversibly oxidized at 500 and 920 mV vs Ag/AgCl reference; -linear analytical range of 10 to 380 mM; -LOD 2.5 mM; -LOQ 8.3 mM;	[132]
11.	β -carotene	Square-wave voltammetry;	-paraffin impregnated graphite electrode;	-supporting electrolyte: 0.1 M HClO ₄ ; -pulse amplitude 50 mV; -step potential 2 mV; -SWV showed oxidation peaks at 0.88 V and 1.09 V versus Ag/AgCl for β -carotene and astaxanthin; -analysis of raw vegetables and fruits;	[133]
12.	β -carotene	Chronoamperometry;	-stochastic sensor based on a graphene-porphyrin composite;	-supporting electrolyte: Acetate buffer pH = 3.0 -working potential of 125 mV versus Ag/AgCl; -linear response in the range between 1.0×10^{-15} mol L ⁻¹ and 1.0×10^{-3} mol L ⁻¹ ; -LOQ 1.0×10^{-15} mol L ⁻¹ ; -sensitivity 8.66×10^{10} s ⁻¹ /mol L ⁻¹ ; -analysis of soft drinks;	[134]
13.	Astaxanthin	Square-wave voltammetry;	-paraffin-impregnated graphite rod electrode	-two electrolyte solutions: 0.1 mol L ⁻¹ HClO ₄ and 0.1 mol L ⁻¹ KNO ₃ ; -frequency of 100 Hz, pulse amplitude 50 mV and step potential 2 mV. -LOD 15.77 μ mol L ⁻¹ and LOQ 47.80 μ mol L ⁻¹ ; -first reversible oxidation at -0.276 V vs. Ag/AgCl; second, not well defined, oxidation peak at -0.032 V; third reversible voltammetric response at 0.335 V;	[135]

Table 2. Cont.

No	Antioxidant	Analytical Method	Carbon-Based Working Electrode	Analytical Characteristics	Ref.
14	Quercetin, dihydroquercetin, ferulic acid, synapic acid, gallic acid, caffeic acid etc.	Cyclic voltammetry;	-pyrographite electrode;	-determinations performed in: 0.2 M potassium phosphate buffer pH 6.0; 0.05 M potassium citrate buffer pH 5.0, and 0.1 M citrate-phosphate buffer pH 3.5; for increasing conductivity, 0.1 M KCl was added as an auxiliary electrolyte; -scanning speed 25 mV/s; -analyzed phenolics showed oxidation peaks in the range 235–834 mV, vs. Ag/AgCl;	[136]
15.	Catechin, caffeic acid, coumaric acid, syringic acid, quercetin, mailvidin trans-resveratrol; estimation of total polyphenols levels;	Cyclic voltammetry;	-glassy carbon electrode	-determinations performed in model wine solution, consisting of 12% (v/v) ethanol, 33 mM l-tartaric acid, pH = 3.0, with Ag/AgCl as reference; -the anodic peak area in the range –100 to 1200 mV accounted for about 70% of total phenolics that absorbed at 280 nm; -catechol and galloyl containing polyphenols present in wine were quantitated relying on the size of the first anodic peak at around 450 mV after treatment with acetaldehyde; -flavonols were quantitated on the basis of the anodic peak current at 1120 mV; -good correlation of total flavanols with HPLC;	[137]
16.	Catechin; estimation of total polyphenols levels;	Differential pulse voltammetry;	-glassy carbon electrode modified with green apple-sourced polyphenol oxidase (biosensor);	-supporting electrolyte phosphate buffer pH 7.65; -the anodic peak for reversible catechin oxidation, noticed at 0.219 V, with a cathodic peak at 0.128 V vs Ag/AgCl reference; -LOD 1.76 $\mu\text{g L}^{-1}$; -LOQ 5.86 $\mu\text{g L}^{-1}$; -RSD 2.5%; -detection of polyphenols in wine;	[138]
17	α -tocopherol;	Square-wave voltammetry;	-carbon fiber disk ultramicroelectrode	-determinations performed in benzene/ethanol and 0.1 mol L ⁻¹ H ₂ SO ₄ ; -square wave amplitude 50 mV; -staircase step height 0.005 V; -frequency 25 Hz; -peak potential between 0.6 and 0.7 V versus SCE;	[139]
18.	α -tocopherol;	Cyclic voltammetry;	-glassy carbon electrode	-supporting electrolyte: Glacial acetic acid and acetonitrile, containing 0.4 M sodium perchlorate; -100 mV s ⁻¹ scan rate; -external silver chloride reference; -peak potential 548 mV at first electron loss (that leads to phenoxyl radical) and 517 mV for second electron loss (that leads to phenoxonium cation radical);	[140]

Table 2. Cont.

No	Antioxidant	Analytical Method	Carbon-Based Working Electrode	Analytical Characteristics	Ref.
19.	α -tocopherol; Gallic acid; ascorbic acid;	Cyclic voltammetry;	-hydrophilic indium tin oxide electrode, lipophilic fluorinated nanocarbon film electrode and glassy carbon electrode;	-supporting electrolyte: Phosphate buffer saline (pH = 7.0), sodium dodecyl sulfate surfactant, 2-butanol cosurfactant, and toluene; -antioxidants analyzed in bicontinuous microemulsion, in which water and oil phases coexisted at microscopic scale; -using the indium tin oxide electrode, hydrosoluble gallic acid, ascorbic acid, and amphiphilic trolox exhibited irreversible anodic oxidation peaks at 0.61, 0.41, and 0.72 V, respectively, vs saturated calomel; -using the lipophilic fluorinated nanocarbon film electrode, amphiphilic trolox and lipophilic α -tocopherol, gave irreversible oxidations at 0.90 and 0.69 V, respectively, vs saturated calomel;	[141]
20.	α -tocopherol;	Square wave anodic stripping voltammetry;	-glassy carbon paste electrode,	-supporting electrolyte: 0.1 M HNO ₃ ; -linear ranges of $5 \times 10^{-7} - 4 \times 10^{-5}$ and $5 \times 10^{-8} - 1 \times 10^{-5}$ mol L ⁻¹ ; -LOD of 1×10^{-7} mol L ⁻¹ ; -anodic peak potential at 520 mV vs. Ag/AgCl reference, -analyte extracted into glassy carbon paste electrode with 10% silicone oil, from 60% aqueous-acetonic mixture; -analysis of margarine and edible oils;	[142]
21.	Superoxide dismutase;	Amperometry;	-glassy carbon electrode;	-detection performed at 0.0 V vs saturated calomel reference -LOD 8×10^{-11} M at pH 7.0, and 2×10^{-12} M at pH 9.0; -assay of buttermilk-sourced superoxide dismutase solution, in 0.1 M phosphate buffer, pH 8.0, containing 1×10^{-4} M EDTA;	[143]
22.	Superoxide dismutase;	Cyclic voltammetry;	-screen-printed carbon electrode modified with self-assembled monolayers of gold nanoparticles in electropolymerized polypyrrole, and biofunctionalized with monoclonal anti-SOD1 antibody (immunosensor);	-supporting electrolyte: 0.1 M phosphate buffer solution containing 100 μ M nitrite; -scan rate of 50 m Vs ⁻¹ , using Ag/AgCl reference; -peak current recorded at the potential 0.8 V for UV-A treated cells was significantly higher than for control cells; -linear working range 0.5 nM to 5 μ M -LOD 0.5 nM; -analysis of cultured human epidermal keratinocytes;	[144]

Table 2. Cont.

No	Antioxidant	Analytical Method	Carbon-Based Working Electrode	Analytical Characteristics	Ref.
23.	Superoxide dismutase;	Cyclic voltammetry; Electrochemiluminescence: Based on the signal (originating from the superoxide anion radical) emitted by methylcypridinalucifrin analogue at the electrode;	-glassy carbon electrode modified with a composite consisting of ferrocene imidazolium salts and hydroxy-functionalized graphene, in a Nafion matrix;	-supporting electrolyte: Phosphate buffer pH 5.3; -peak accounting for superoxide dismutase activity present between 0.6 and 0.7 V in electrochemiluminescence, and between 0.7 and 0.8 in cyclic voltammetry; -calibration plot linear in the 0.5 to 6.5 U·mL ⁻¹ SOD activity range, with LOD = 0.2 U·mL ⁻¹ in electrochemiluminescence; light emission lowered as SOD activity increased, correlated with oxygen generation from superoxide. -RSD (n = 11) 2.3% for 2.0 U·mL ⁻¹ SOD in electrochemiluminescence; -scan range between 1.0 and -1.2 V vs. Ag/AgCl in cyclic voltammetry and electrochemiluminescence -scan rate: 0.1 V·s ⁻¹	[145]
24.	Glutathione;	Cyclic voltammetry; Amperometry; Differential pulse voltammetry;	-multiwalled carbon nanotubes@reduced graphene oxide nanoribbons core-shell heterostructure-modified glassy carbon electrode;	-supporting electrolyte: 0.01 M phosphate buffered saline, pH 7.0; -CV measurements carried out from -0.2 V to +0.6 V, or from +0.3 V to +0.8 V at a scan rate of 50 mV s ⁻¹ , showing enhanced electrocatalytic activity for the developed electrode; -DPV measurements carried out by scanning from +0.2 V to +0.7 V at a pulse amplitude of 50 mV; -highest voltammetric response obtained at 0.55 V vs. Ag/AgCl; -amperometric measurements carried out in 0.01 M phosphate buffer pH 7.0 at +0.55 V vs. Ag/AgCl; -LOD 0.039 μM (amperometry); -two linear ranges: 0.05–266.3 μM and 266.3–766.3 μM (amperometry); -RSD 3.53% (amperometry); -analysis of real human serum samples;	[146]
25	Glutathione;	Cyclic voltammetry; Square wave voltammetry;	-gold-copper metal-organic framework immobilized on the surface of a glassy carbon electrode;	-supporting electrolyte: 0.1 mol L ⁻¹ phosphate buffer, pH 3.0; -anodic oxidation peak appeared at around +0.30 V vs. Ag/AgCl in CV and +0.25 V vs. Ag/AgCl in SWV; -linear dynamic range 1–10 μmol L ⁻¹ in SWV; -LOD 0.30 μmol L ⁻¹ in SWV; -sensitivity 0.89 ± 0.02 μA μmol L ⁻¹ in SWV; -repeatability 2.14% in SWV; -analysis of commercial tablets with more than 98% recovery;	[147]

Table 2. Cont.

No	Antioxidant	Analytical Method	Carbon-Based Working Electrode	Analytical Characteristics	Ref.
26.	Glutathione; Glutathione disulphide;	Cyclic voltammetry; Square-wave voltammetry;	-antimony trioxide-modified-carbon paste electrode;	-supporting electrolyte: 0.2 mol/L Britton-Robinson buffer; -oxidation potentials of +1.08 V for glutathione and +1.36 V for oxidized glutathione, vs. Ag/AgCl reference in CV and SWV; -SWV responses linear in the concentration range of 2 to 300 $\mu\text{mol/L}$ glutathione; -LOD of 0.34 $\mu\text{mol/L}$ glutathione and 0.1 $\mu\text{mol/L}$ for oxidized glutathione in SWV; -determination of glutathione and glutathione disulphide in urine samples; -ascorbic acid, cysteine, glucose, glutamic acid and uric acid gave no significant interferences;	[148]
27.	Uric acid;	Cyclic voltammetry; Chronoamperometry;	-glassy carbon electrode, modified with a ZnO/carboxylic acid/multiwalled nanotube composite;	-supporting electrolyte: Phosphate buffer solution, pH = 7.0; -cyclic voltammetric peak at 0.5 V vs. Ag/AgCl; -chronoamperometric measurements performed at +0.577 V vs. Ag/AgCl; -rapid current response time (<5 s); -selective measurement of uric acid at clinically relevant concentrations (100–900 μM) by chronoamperometry;	[149]
28.	Uric acid;	Cyclic voltammetry; Differential pulse voltammetry;	-ZnO nanorods and graphene nanosheets hybrid electrode sprayed on indium tin oxide (ITO) glass;	-supporting electrolyte: Phosphate buffer saline, 0.01 M, pH = 7.4; -potential range: -0.2 to 0.6 V, vs. Ag/AgCl reference electrode (CV and DPV); -CVs were recorded at a scan rate of 50 mV s^{-1} ; -cyclic voltammetric oxidation peak potentials of uric acid and ascorbic acid, were 0.36 V and 0.28 V, respectively, -DPV analytical responses recorded with: A pulse height of 50 mV, a step height of 4 mV, a pulse width of 0.2 s, and a step time of 0.5 s; -sensitivity for uric acid $0.3 \mu\text{A } \mu\text{M}^{-1} \text{ cm}^{-2}$ (DPV); -peak current intensities linearly related to the uric acid concentration in the range of 5–80 μM (DPV); -LOD 5 μM (DPV); -potentially applicable to clinical determination of uric acid;	[150]
29.	Uric acid;	Cyclic voltammetry;	uricase/carboxymethylcellulose dispersed carbon nanotube/gold thin film biosensor;	-supporting electrolyte: 0.05 M phosphate buffer solution (pH 7.4); -cyclic voltammetric sweep rate: 50 mV s^{-1} ; -sensitivity of $233 \mu\text{A mM}^{-1} \text{ cm}^{-2}$ at +0.35 V vs. Ag/AgCl reference; -linear range 0.02–2.7 mM; -detection limit of 2.8 μM ; -detection of uric acid in serum and urine; -negligible interferents effect from urea and ascorbic acid at physiological amounts;	[151]

Table 2. Cont.

No	Antioxidant	Analytical Method	Carbon-Based Working Electrode	Analytical Characteristics	Ref.
30.	Bilirubin;	Cyclic voltammetry; Amperometry;	-carbon electrode modified with multiwalled carbon nanotubes or electrochemically reduced graphene oxide;	-supporting electrolyte: 0.1 M phosphate buffer solution (pH 7.2); -scan rate of 50 mV s ⁻¹ ; -two cyclic voltammetric oxidation peaks: At +0.25 V, corresponding to the oxidation of bilirubin to biliverdin and another at +0.48 V, corresponding to the oxidation of biliverdin to purpurine; -graphene type electrode: Amperometric linear range 0.1–600 μM and LOD 0.1 ± 0.018 nM; sensitivity 30 nA μM ⁻¹ cm ⁻² , at 0.48 V vs. Ag/AgCl reference; -multiwalled carbon nanotube type: Amperometric linear range 0.5–500 μM; LOD 0.3 ± 0.022 μM; sensitivity 15 nA μM ⁻¹ cm ⁻² , at 0.48 V vs Ag/AgCl reference; -no interferences from glucose, ascorbic acid, uric acid, and glutathione; -analysis of blood serum samples;	[152]
31	Bilirubin;	Linear sweep voltammetry; Differential pulse voltammetry;	-disposable screen-printed carbon electrodes obtained using graphite carbon ink printed on a PET substrate;	-supporting electrolyte: 0.05 M Trizma buffer, pH 8.5; -LSVs were recorded at a potential window of 0 to 0.6 V at a scan rate of 0.1 V/s; -DPVs were obtained at a potential window of 0 to 0.6 V with pulse amplitude of 0.05 V and pulse width of 0.05 s; -two anodic voltammetric peaks noticed on DPVs at around 0.25 V and 0.35 V (vs Ag/AgCl reference) corresponding to the oxidation of bilirubin to biliverdin, and of biliverdin to purpurin; -linear range 5–600 μM (LSV); -sensitivity 95 μA μM ⁻¹ cm ⁻² (LSV); -good selectivity in the presence of glucose, creatinine and ethanol; -application to serum samples;	[153]
32.	Bilirubin;	Cyclic voltammetry; Differential pulse voltammetry;	-carbon paste electrode;	-supporting electrolyte: 0.05 M phosphate buffer solution (pH 8.0); -two step oxidation process at around 300 mV and around 500 mV (CV); -DPV parameters: Pulse time 10 ms, potential step 5 mV and 150 ms optimized pulse amplitude; -linear range 3.5–25 μmol L ⁻¹ in DPV, considering the signal of irreversible anodic oxidation at 320 mV vs. Ag/AgCl; -LOD 1.2 μmol L ⁻¹ in DPV;	[154]

Table 2. Cont.

No	Antioxidant	Analytical Method	Carbon-Based Working Electrode	Analytical Characteristics	Ref.
33.	Melatonin;	Cyclic voltammetry; Fixed-potential amperometry;	-screen-printed carbon electrode modified with graphene;	-supporting electrolyte: 0.1 M phosphate buffer (pH 7.0); -oxidation CV peaks at 0.22 V and 0.80 V; reduction peaks at 0.12 V and 0.75 V vs pseudosilver/silver chloride reference electrode, -linear range of 1–300 μM in amperometry, at 0.8 V; -LOD 0.87×10^{-6} M and LOQ 2.91×10^{-6} M in amperometry; -RSD = 1.24% at the assay of Bien Dormir tablets (CV);	[155]
34.	Melatonin;	Square wave voltammetry;	-glassy carbon electrode;	-linear concentration range of 5–200 μM ; -LOD of 0.3432 μM ; -analytical peak present at about 650 mV; -determination in pharmaceutical formulations and in human urine;	[156]
35.	Melatonin;	Square wave voltammetry;	-carbon fiber microelectrode;	-reliably quantified melatonin concentrations in the visual cortex of anesthetized mice after intraperitoneal injections of different melatonin doses; -SWV enabled sensitive detection of oxidation peak at about 0.7 V vs. Ag/AgCl, discriminating melatonin from most common interferents;	[157]
36.	Coenzyme Q ₁₀ ;	Differential pulse voltammetry;	-glassy carbon electrode;	-supporting electrolyte: Acetic acid containing 20% acetonitrile and 0.5 M CH ₃ COONa; -DPV pulse amplitude of 20 mV, scan rate of 20 mV s ⁻¹ and pulse width of 80 ms allowed both fast recording and good resolution; -well-configured DPV cathodic peak attributed to reduction of CoQ ₁₀ at -20 mV vs. silver chloride external reference -LOD 0.014 mM (12 mg L ⁻¹); -LOQ 0.046 mM (40 mg L ⁻¹); -linearity up to 1 mM, with excellent correlation ($r = 0.9989$); -determination in commercial capsules;	[158]
37.	coenzyme Q ₁₀ ;	Direct current voltammetry;	-glassy carbon electrode;	-supporting electrolyte: Phosphate buffer solution (pH 6.86); -reversible oxidation peak at +0.4 V, corresponding to oxidation of hydroquinone group; reduction peak at -0.6 V vs. silver chloride reference; consistent to the previously confirmed reduction of ubiquinone to ubiquinol; -linear range 2.0×10^{-5} – 2.0×10^{-4} M; -assay of coenzyme Q ₁₀ in pharmaceuticals;	[159]

Table 2. Cont.

No	Antioxidant	Analytical Method	Carbon-Based Working Electrode	Analytical Characteristics	Ref.
38.	Coenzyme Q ₁₀ ; α -lipoic acid;	Cyclic voltammetry; Square wave anodic stripping voltammetry;	-MnO ₂ -modified screen-printed graphene electrodes;	-determinations performed in 20:80 (v/v) ratio of ethanol/acetate buffer 0.1 M at pH 4.0; -the anodic peak of alpha lipoic acid present at a potential of 0.64 V, and that of coenzyme Q ₁₀ at 0.22 V, vs Ag/AgCl paste reference electrode (CV); -optimized square wave parameters: 5 mV step potential, 20 mV amplitude, and 25 Hz frequency; - linear range 2.0–75.0 $\mu\text{g mL}^{-1}$ for coenzyme Q ₁₀ , and 0.3–25 $\mu\text{g mL}^{-1}$ for α -lipoic acid in square wave anodic stripping voltammetry; -LOD 0.56 $\mu\text{g mL}^{-1}$ for coenzyme Q ₁₀ and 0.088 $\mu\text{g mL}^{-1}$ for α -lipoic acid in square wave anodic stripping voltammetry; -determination in dietary supplements with good specificity in the presence of other vitamins and ionic species;	[160]
39.	Vitamin D ₂ and D ₃ ;	Cyclic voltammetry; Differential pulse voltammetry;	-glassy carbon electrode;	-supporting electrolyte: 40% ethanol/60% water containing LiClO ₄ ; -potential range of 0.0 to +1.5 V and scan rate of 50 mV s ⁻¹ (CV); -three well-configured, separate DPV peaks: Vitamin D around 0.594 V, vitamin E around 0.334 V, and vitamin A around 0.841 V vs. Ag/AgCl reference; -LOD 1.3 $\times 10^{-7}$ (vitamin D ₂) and 1.18 $\times 10^{-7}$ mol/L (vitamin D ₃) in DPV; -determination in vitamin D ₃ tablets;	[161]
40.	Vitamin D ₂ and D ₃ ;	Cyclic voltammetry; Differential pulse voltammetry;	-glassy carbon electrode modified with AuPd;	-supporting electrolyte: Ethanol/water (40%/60%: v/v) containing lithium perchlorate; -CV scan rate of 50 mV/s, in the domain 0.0–1.5 V; -DPV scan rate: 10 mV/s, sampling time: 20 ms, pulse interval: 100 ms. -detection potential of +0.4 V vs. Ag/AgCl enabled diminution of interferences and good separation from vitamins A and E (DPV); -linear ranges 1–10 μM vitamin D ₂ , 5–50 μM vitamin D ₃ in DPV; -LOD 0.15 μM vitamin D ₂ and 0.18 μM vitamin D ₃ (DPV); -detection of vitamin D ₃ in drug specimen;	[162]
41.	Vitamin D ₃ ;	Square wave voltammetry;	-boron-doped diamond electrode;	-supporting electrolyte: 0.02 mol L ⁻¹ Britton-Robinson buffer pH 5.0 prepared in 50% ethanol; -well-defined voltammetric peak at around +1.00 V vs. Ag/AgCl; -linear range 2 to 200 mol L ⁻¹ ; -LOD 0.17 $\mu\text{mol L}^{-1}$; -LOQ 0.51 $\mu\text{mol L}^{-1}$; -determination in pharmaceutical products;	[163]

Table 2. Cont.

No	Antioxidant	Analytical Method	Carbon-Based Working Electrode	Analytical Characteristics	Ref.
42.	Alpha lipoic acid;	Cyclic voltammetry; Chronoamperometry; Differential pulse voltammetry;	-pyrolytic graphite electrode modified with cobalt phthalocyanine;	-supporting electrolyte: Phosphate buffer solution (pH = 7.0); -scan rate (CV) 25 m Vs. ⁻¹ ; -oxidation peak present at 0.84 V vs. SCE (CV), with highest response resulted from modification with cobalt phthalocyanine; -LOD 2.5×10^{-7} mol L ⁻¹ and LOQ 8.3×10^{-7} mol L ⁻¹ (CV); -LOD 9.8×10^{-8} mol L ⁻¹ and LOQ 3.2×10^{-7} mol L ⁻¹ (Chronoamperometry); -LOD 3.4×10^{-9} mol L ⁻¹ and LOQ 1.2×10^{-8} mol L ⁻¹ (DPV); -determination in pharmaceutical dietary supplement samples;	[164]
43.	Alpha lipoic acid;	Amperometry;	-cobalt phthalocyanine-modified pyrolytic graphite electrode, integrated in a batch injection analysis set-up;	-supporting electrolyte: 0.1 mol L ⁻¹ phosphate buffer, pH 7.0; -applied potential of 0.9 V vs. Ag/AgCl; -linear response in the range 1.0×10^{-5} – 1.3×10^{-4} mol L ⁻¹ ; -LOD 1.5×10^{-8} mol L ⁻¹ ; -quantification in dietary supplements and in synthetic urine;	[165]
44.	Alpha lipoic acid;	Cyclic voltammetry; Differential pulse voltammetry;	-SnO ₂ nanoparticles-modified glassy carbon electrode;	-supporting electrolyte: Britton-Robinson buffer pH 4.5; -well-defined DPV oxidation peak at 0.843 V vs. Ag/AgCl; -two linear dynamic ranges of 0.50–50 and 50–400 μmol L ⁻¹ (DPV); -LOD 0.13 μmol L ⁻¹ (DPV); -LOQ 0.43 μmol L ⁻¹ (DPV); -analysis of pharmaceutical dosage forms, with RSD between 0.45 and 6.2%;	[166]
45.	Tert-butylhydroquinone and butylated hydroxyanisole	Cyclic voltammetry; Square-wave voltammetry;	-carbon black paste electrode;	-optimum conditions of electrolyte: 0.2 mol L ⁻¹ phosphate buffer (pH 7.0), 600.0 μmol L ⁻¹ surfactant cetylpyridinium bromide; -scan rate 50.0 mVs ⁻¹ ; -anodic cyclic voltammetric peak at cca 0 V vs. Ag/AgCl for tert-butylhydroquinone and at 0.4 V for butylated hydroxyanisole; -LOQ for tert-butylhydroquinone 0.23 μmol L ⁻¹ (SWV) and 0.27 μmol L ⁻¹ (DPV); -LOQ for butylated hydroxyanisole 0.26 μmol L ⁻¹ (SWV) and 0.23 μmol L ⁻¹ (DPV); -determination in mayonnaise, margarine, biodiesel;	[167]

A series of irreversible cyclic voltammograms recorded for increasing ascorbic acid concentrations, at a carbon paste electrode are given in Figure 1.

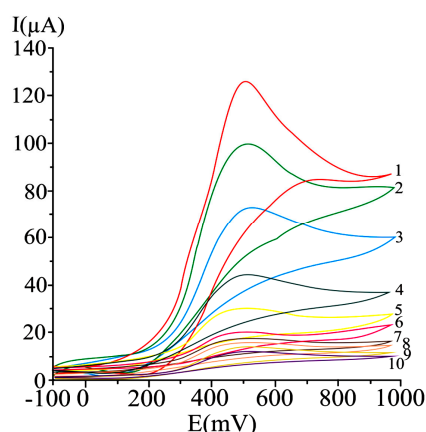


Figure 1. Cyclic voltammograms obtained at a carbon paste working electrode at varying ascorbic acid concentrations, as mM: 20 (1), 15 (2), 10 (3), 5 (4), 2.5 (5), 1.25 (6), 0.625 (7), 0.31 (8), 0.15 (9), and 0.07 (10); potential scan rate 50 mV/s [123].

A 50 mV s^{-1} cyclic voltammetric scan rate could enable analyte diffusion to the electrode and promoted electron transfer. In the case of irreversible or quasi-reversible voltammograms [123,168], at elevated scan rates, electron transfer is slow relative to the applied potential sweep rate, so the rate of establishing the equilibrium at the electrode is diminished. In the case of very elevated scan rates, peaks have high current intensities, but distortions may occur on the voltammogram [168]. In differential pulse voltammetry at carbon paste electrode (Figure 2), the optimum value of 75 mV was used for the pulse amplitude, and 125 ms was chosen for the pulse period, allowing a good compromise between promoting analytical signal, minimizing noise and good resolution [123].

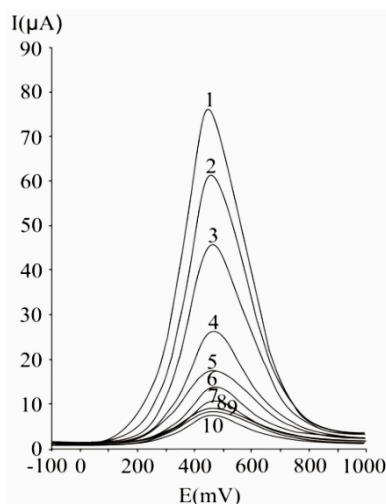


Figure 2. Differential pulse voltammograms obtained with a carbon paste working electrode for different ascorbic acid concentrations, expressed as mM: 20 (1), 15 (2), 10 (3), 5 (4), 2.5 (5), 1.25 (6), 0.625 (7), 0.31 (8), 0.15 (9), and 0.07 (10); experimental conditions: Pulse amplitude 75 mV, pulse period 125 ms, potential scan rate 50 mV/s [123].

4. Determination of Total Antioxidant Activity with Carbon-Based Electrodes

Bare and modified carbon-based electrodes have been used for the antioxidant activity and its main contributors' assessment. The electrochemical measurements are performed as per reference to a standard antioxidant, Trolox, gallic acid, ascorbic acid or quercetin, etc. In most of the cases, the peak intensities or peak areas are considered, providing quantitative informations.

Often, authors report indexes illustrating antioxidant activity: IC₃₀ and IC₅₀ [169]. IC₅₀ corresponds to the antioxidant amount that induces a change of a model signal by 50%. The lower the concentration required for 50% increase or inhibition of the considered model signal, the more active the antioxidant. Korotkova et al. [170] relied on the modifications in the oxygen electro-reduction current in the presence of antioxidants, as criteria to determine IC₅₀ by voltammetry. Catalase and superoxide dismutase yielded an increase of the oxygen electro-reduction current, when compared to the signal obtained in supported electrolyte. Superoxide dismutase presented an IC₅₀ value of 1.08 μM [170]. Wei et al. evaluated IC₅₀, as the antioxidant amount that diminishes the oxidation peak of superoxide by 50%. They reported an IC₅₀ value of ascorbic acid of 5×10^{-4} mol/L [171].

Blasco et al. [172] define the “Electrochemical Index” as the total polyphenolic content measured by an electrochemical technique. In this approach, the corresponding total phenolics concentration obtained from the “total electrochemical signal” was named “Electrochemical Index”. The total electrochemical signal was assimilated to the total amperometric current measured at controlled potential (800 mV), to achieve oxidation of all polyphenolics at neutral pH of 7.5. So, the “Electrochemical Index” became an approach to “total polyphenols” in samples without ascorbic acid (or alpha-tocopherol), or an approach to “total natural antioxidant” content in those samples where ascorbic acid (or alpha-tocopherol) could be present [172].

An overview of the analytical parameters and real sample applications regarding the assay of total antioxidant activity by the use of carbon-based working electrodes is given in Table 3 [173–205].

Table 3. Some relevant examples of electrochemical assay of antioxidant activity and its key contributors [173–205].

No.	Analytical Method	Carbon-Based Working Electrode	Analytical Characteristics	Ref.
1.	Cyclic voltammetry; Chronoamperometry; Square-wave voltammetry;	-poly(gallic acid)/multiwalled carbon nanotube modified glassy carbon electrode;	-supporting electrolyte 0.2 M H ₃ PO ₄ ; -cyclic voltammetric scan rate 50 mV/s; -catalytic rate constant of 2.75×10^4 mol L ⁻¹ s ⁻¹ , in chronoamperometry; -voltammetric oxidation peak for gallic acid at 0.53 V vs Ag/AgCl, in CV and SWV; -linear range of 4.975×10^{-6} to 3.381×10^{-5} M (SWV); -LOD 3.22×10^{-6} M gallic acid (SWV); -the SWVs of a fresh pomegranate juice sample shows three anodic peaks at 0.60, 0.70 and 1.0 V; signals can be attributed to the oxidation of different polyphenolic compounds, including gallic acid and catechin; -determination of total phenolic content in pomegranate juice, as gallic acid equivalent; -lack of interference of ascorbic acid, fructose, potassium nitrate and barbituric acid;	[173]
2.	Cyclic voltammetry; Differential pulse voltammetry;	-nanocarbon-nanosilver hybrid electrode;	-supporting electrolyte: Phosphate buffer solution, pH 7.0; -CV studies confirmed that silver nanoparticles were efficiently immobilized on the Printex carbon surface; anodic and cathodic peak potentials noticed, were assigned to the redox pair Ag ⁰ /Ag ⁺ , whose presence was confirmed in the nanocomposite’s structure; -DPV peak of gallic acid at 0.091 V vs. Ag/AgCl; -sensitivity 0.254 μA/mol L ⁻¹ in DPV; -LOD 0.0663 μM in DPV; -linear range 5.0×10^{-7} – 8.5×10^{-6} in DPV; -estimation of antioxidant activity in wine;	[174]

Table 3. Cont.

No.	Analytical Method	Carbon-Based Working Electrode	Analytical Characteristics	Ref.
3.	Cyclic voltammetry; Amperometry;	-single-walled carbon nanotubes electrode, covalently functionalized with polytyrosine;	-supporting electrolyte 0.050 M phosphate buffer solution, pH 7.40; -CVs recorded between -0.200 V and 0.800 V (vs. Ag/AgCl) at a scan rate of 0.100 V s ⁻¹ ; -cyclic voltammetric oxidation peak potential for gallic acid at 0.2 V; -amperometric working potential 0.200 V; -amperometric sensitivity 163.2 mA/mol L ⁻¹ ; -amperometric LOD 8.8×10^{-9} M; -quantification of polyphenols in tea extracts: Green-Patagonia, red-Patagonia, classic-Green Hill and herbal (Taragüü);	[175]
4.	Differential pulse Voltammetry;	-TiO ₂ nanoparticles/multiwalled carbon nanotubes-modified glassy carbon electrode; -guanine biosensor based on TiO ₂ nanoparticles and multiwalled carbon nanotubes, immobilized on glassy carbon electrode;	-supporting electrolyte: phosphate buffer solution, pH 7.4; -oxidation DPV peak at 0.80 V (vs. SCE) corresponding to the electro-oxidation of guanine at the developed biosensor; -the peak intensity value of guanine oxidation increased linearly with increasing metabisulfite (employed as OH radical scavenger) concentration from 1 to 30 mmol L ⁻¹ ; -LOD 0.54 mmol L ⁻¹ for the guanine biosensor; -quantification of the antioxidant capacity in drug samples (adrenaline hydrochloride injection);	[176]
5.	Cyclic voltammetry; Differential pulse Voltammetry;	-carbon paste electrode;	-supporting electrolyte: 0.1 M phosphate buffer, pH 5.0; -a cyclic voltammetric anodic peak at 0.33 V, with a corresponding cathodic peak at 0.28 V, vs Ag/AgCl, for 1% coffee sample in 0.1 M phosphate buffer pH 5.0; -two further anodic peaks at 0.55 V and 0.78 V were observed in DPVs of 0.5% coffee sample, in the same electrolyte; -good correlation with DPPH photometry and HPLC; -evaluation of the antioxidant activity of roasted coffee samples; -determination of electrochemical index of roasted coffee samples on the basis of the sum of the ratios of anodic peak currents to anodic peak potentials noticed on DPVs;	[177]

Table 3. Cont.

No.	Analytical Method	Carbon-Based Working Electrode	Analytical Characteristics	Ref.
6.	Cyclic voltammetry; Square-wave voltammetry; Chronoamperometry	-nanocomposite-graphene/poly (3,4-ethylenedioxythiophene); Poly (styrenesulfonate) modified screen-printed carbon electrode;	<p>-supporting electrolyte: Ethanolic phosphate buffer solution based on 60% ethanol and 0.1 M phosphate buffer saline, pH 7.0;</p> <p>-method relied on DPPH reduction by antioxidants;</p> <p>-the presence of Trolox yielded a well-countoured anodic peak at around 0.9 V and a small cathodic peak at 0.3 V.</p> <p>-cathodic cyclic voltammetric peak potentials of catechin and caffeic acid were present at -0.03 V and -0.025 V vs. Ag/AgCl;</p> <p>-square voltammetric peak of DPPH at 0.25 V;</p> <p>-chronoamperometric DPPH detection at 0.2 V vs. Ag/AgCl; the linear calibration between the difference of cathodic DPPH currents (in the presence and absence of standard Trolox solution) and Trolox concentration in a range of 5–30 μM;</p> <p>-LOD 0.59 μM and LOQ 1.97 μM (chronoamperometry);</p> <p>-RSD of reproducibility is 2.13% (chronoamperometry);</p> <p>-RSD of repeatability 2.78% (chronoamperometry);</p> <p>-evaluation of the antioxidant activity in Thai herb and herbal beverage, expressed as mg of Trolox/g of sample;</p>	[178]
7.	Differential pulse voltammetry;	-multi-walled carbon nanotubes-modified glassy carbon electrode;	<p>-supporting electrolyte: 0.1 M phosphate buffer (pH 4.0–7.0);</p> <p>-three DPV oxidation peaks observed at 0.39, 0.61 and 0.83 V for red dry wine and at 0.39, 0.80 and 1.18 V vs. Ag/AgCl for white dry wine, in phosphate buffer pH 4.0;</p> <p>-RSD% (as gallic acid equivalents) comprised between 1.0 and 6.9, as function of the wine sample;</p> <p>-evaluation of red and white dry wine antioxidant capacity, as gallic acid equivalents per 1 L of wine;</p>	[179]
8.	Differential pulse voltammetry;	-carbon paste electrode; -laccase-based modified carbon paste biosensor for the determination of phenolic content;	<p>-supporting electrolyte: 0.1 mol L⁻¹ phosphate buffer, pH 6.0;</p> <p>-biosensor was characterized by enhanced activity in mild acid medium and the response time (corresponding to the time required for enzyme oxidation of phenolic compounds), was lower than 30 s, but gradually increased up to 240 s, when a plateau was reached;</p> <p>-honey samples presented 2 to 3 anodic DPV peaks, the first at about 0.2 V, the second at about 0.5 V and the third nearby 0.8 V vs. Ag/AgCl;</p> <p>-electrochemical index determination, based on the sum of ratios of peak currents to peak potentials;</p> <p>-determination of phenolic content in honey samples;</p>	[180]

Table 3. Cont.

No.	Analytical Method	Carbon-Based Working Electrode	Analytical Characteristics	Ref.
9.	Cyclic voltammetry; Differential pulse voltammetry;	-carbon black nanoparticles press imprinted films;	<ul style="list-style-type: none"> -supporting electrolyte: Phosphate buffer pH 7.40; -scan rate of 50 mV s⁻¹ in the potential range of -0.20 V to +1.0 V vs. Ag/AgCl (CV); -pulse amplitude 50 mV/s, scan rate 10 mVs⁻¹ (DPV); -anodic peaks of o-diphenols and m-phenols present in olive oil extract, noticed in the range 0.120–0.160 V and 0.590–0.610 V (vs. Ag/AgCl), respectively; consistency with results obtained for the standards (DPV); -good repeatability for o-phenols; -RSD < 6% (o-phenols), RSD < 15% (m-phenols) in CV; -stable and reproducible voltammetric response of carbon black nanoparticles-based electrode; -determination of phenolic content and electrochemical indexes in olive oil extracts, using hydroxytyrosol and tyrosol as standards; 	[181]
10.	Cyclic voltammetry; Differential pulse voltammetry;	-glassy carbon electrode;	<ul style="list-style-type: none"> -supporting electrolyte: Dimethylsulfoxide, with tetrabutylammonium hexafluorophosphate 0.1 mol L⁻¹; -the CVs were obtained at a scan rate of 100 mV s⁻¹; -DPV pulse width = 5 mV, pulse amplitude = 60 mV and scan rate = 20 V s⁻¹; -oxidation of ascorbic acid at 0.90 V in cyclic voltammetry and around 0.75 V vs. Ag/AgCl in differential pulse voltammetry; -in the CVs of the bark extract, a very well contoured peak was observed at 1.3 V, corresponding to meta-diphenols and isolated phenols; -in the CVs of the root and leaf extracts, an additional peak at 0.9 V indicates the presence of phenolics with ortho- or para-diphenol groups, in low amounts; -determination of the antioxidant capacity of <i>Bunchosia glandulifera</i> (Jacq.) Kunth (Malpighiaceae) extracts, using ascorbic acid as standard; 	[182]
11.	Chrono-amperometry; Differential pulse voltammetry;	-glassy carbon electrode modified with multi-walled carbon nanotubes; -glassy carbon polyquercetin-modified electrode;	<ul style="list-style-type: none"> -supporting electrolyte: Phosphate buffer pH 7.0; -antioxidant capacity using gallic acid as reference; -DPVs recorded from 0 to 0.8 V (pulse amplitude 50 mV, pulse time 50 ms and potential scan rate 10 mV/s); -DPVs of tea on the polyquercetin-modified electrode exhibited oxidation peaks at 0.080 and 0.19 V depending on the type of tea and a less configured oxidation step between 0.55 and 0.62 V vs Ag/AgCl; -chronoamperograms recorded at a constant potential of 0.2 V, potential corresponding to oxidation of tea antioxidants; -RSD = 0.5–20%, as function of the tea type (chronoamperometry); -determination of the antioxidant capacity of tea, highest content for Green Sencha; 	[183]

Table 3. Cont.

No.	Analytical Method	Carbon-Based Working Electrode	Analytical Characteristics	Ref.
12.	Cyclic voltammetry;	-glassy carbon electrode;	-supporting electrolyte: Phosphate buffer pH = 7.0; -cyclic voltammetric scans performed between 0.0 and 0.5 V vs Ag/AgCl at a scanning rate of 5 mV/s; -anodic peak at 244 mV for pomace and its parts (skins and stems), and 252 mV for seeds; -analyse of winemaking by-products (pomace, skins, seeds and stems separated from pomace);	[184]
13.	Cyclic voltammetry;	-glassy carbon electrode;	-supporting electrolyte: 0.1 M sodium acetate–acetic acid buffer at pH 3.6; -all the grapes revealed peak I at 0.26–0.31 V, peak II between 0.42 and 0.55 V, and peak III at approximately 0.66 V vs Ag/AgCl; -correlations of anodic peak area with phenolic content and antioxidant activity were assessed; -determination of phenolic contents and antioxidant capacity in 12 grape cultivars;	[185]
14.	Cyclic voltammetry; Square-wave voltammetry; Differential pulse voltammetry	-glassy carbon electrode; -laccase-modified carbon paste electrode;	-supporting electrolyte: 0.1 M phosphate buffer solution, pH 6.0, using Ag/AgCl reference; -CV: Scan rate of 100 mV s ⁻¹ within the range 0–1.4 V; -SWV: Pulse amplitude 50 mV, frequency 50 Hz and a potential increment of 2 mV, scan rate of 100 mV s ⁻¹ ; -first peak present between 100 and 400 mV, second between 0.55 and 0.7, and third at around 1 V, in CV/SWV; -solutions of the extracts yielded highest DPV peaks at 0.2 V, alongside peaks present at 0.6 and 0.9 V; -electrochemical indexes were calculated based on the sum of ratios of peak currents to peak potentials in DPV; -antioxidant activity evaluation of dried herbal extracts; -highest electrochemical indexes obtained for <i>Gingko biloba</i> and <i>Hypericum perforatum</i> , consistent with the results obtained by spectrophotometry;	[186]
15.	Cyclic voltammetry; Differential pulse voltammetry;	-glassy carbon electrode;	-supporting electrolyte 0.1 M KCl; -CV scan from 0 to +1000 mV at a scan rate of 100 mV s ⁻¹ ; -DPV scan from 0 to +1000 mV at a scan rate of 100 mV s ⁻¹ ; -the first peak of mature-phase milk occurred at around 400 mV; colostrum, had oxidation peaks at very high potential, around 800 mV (DPV) vs Ag/AgCl; -mature-phase milk yielded a peak at around 400 mV; pasteurized milk had a peak at around 500 mV (CV); -areas below oxidation peaks proportional to the amount of antioxidant compounds; -free radical scavenging activity was highest for fresh breast milk and lowest for pasteurized breast milk, confirming the results obtained in DPPH assay; -correlation between DPV and CV ($r = 0.602$, $p < 0.001$); correlation between DPV and DPPH method ($r = 0.339$, $p = 0.003$); correlation between CV and DPPH method ($r = 0.468$ $p < 0.000$);	[187]

Table 3. Cont.

No.	Analytical Method	Carbon-Based Working Electrode	Analytical Characteristics	Ref.
16.	Cyclic voltammetry; Differential pulse voltammetry;	-screen-printed carbon electrodes;	<ul style="list-style-type: none"> -supporting electrolyte 0.1 M HCl; -in CV, the potential recorded between 0.0 V and +1.2 V, at 100 mV s⁻¹ scan rate, using silver pseudo-reference electrode; -optimum DPV parameters: 100 mV modulation amplitude, 10 mV step potential, 0.05 s modulation time and 0.5 s interval time; -ortho-diphenols (oleuropein, hydroxytyrosol and caffeic acid) show one anodic peak between 0.5 and 0.6 V, and one cathodic peak between 0.4 and 0.6 V (CV); same compounds present an anodic peak at +0.5 V, in standard and real sample (DPV); -ferulic acid gave an oxidation peak at higher potential (0.7 V), in the standard solution, whereas this signal was almost negligible in the real sample (DPV); -tyrosol is oxidized at +0.93 V, alongside other mono-phenols (such as vanillic acid) that suffer oxidation around this potential value, in standard and real sample (DPV); -LOD of 0.022 mg L⁻¹ for caffeic acid and tyrosol, in DPV; -determination of hydrophilic phenols in olive oil; 	[188]
17.	Cyclic voltammetry; Differential pulse voltammetry; Square-wave voltammetry;	-electroactivated pencil graphite electrode;	<ul style="list-style-type: none"> -supporting electrolyte: 0.05 mol L⁻¹ potassium hydrogen phthalate; -naringenin is irreversibly oxidized, giving rise to two pH-dependent peaks due to mixed (diffusion- and adsorption-controlled) electrode processes involving two electrons and one proton; -LOD = 3.06 × 10⁻⁸ mol L⁻¹, and LOQ = 1.02 × 10⁻⁷ mol L⁻¹ for DPV, expressed as naringenin; -LOD = 4.40 × 10⁻⁸ mol L⁻¹, and LOQ = 1.11 × 10⁻⁷ mol L⁻¹ for SWV, expressed as naringenin; -application to determination of polyphenol content in citrus juice; 	[189]
18.	Amperometry; Cyclic voltammetry;	-disposable polyester screen-printed graphitic macroelectrodes;	<ul style="list-style-type: none"> -supporting electrolyte: 1:1 (v/v) methanol: Ethanol mixture containing 0.05 mol/L⁻¹ LiCl; -CV scans between -0.3 and +1.0 V, scan rate 50 mV s⁻¹, for DPPH 1 mmol/L⁻¹ (in 50 mmol L⁻¹ LiCl prepared in methanol:ethanol) and for DPPH in the presence of antioxidants; -chlorogenic acid, caffeic acid, catechin and quercetin were oxidized between +0.7 and +0.9 V (CV); -oxidation processes of tocopherol and BHT occurred at more positive potentials, around +1.0 V (CV); -amperometric detection of DPPH remaining after reaction with antioxidants, at +0.1 V (vs. pseudo AgCl). -analysis of edible oils; 	[190]

Table 3. Cont.

No.	Analytical Method	Carbon-Based Working Electrode	Analytical Characteristics	Ref.
19.	Cyclic voltammetry; Differential pulse voltammetry; Linear sweep voltammetry;	-multi-walled carbon nanotube paste electrode;	-supporting electrolyte: 0.02 M acetate-acetic acid buffer/4% methanol (pH 4.5); -CV scan between 0 and 1.5 V, at 100 mV s ⁻¹ ; -DPV pulse amplitude 50 mV and scan rate 100 mV s ⁻¹ -CV oxidation potential at 1.12 V; -DPV oxidation potential at 1.19 V; -the average Tafel slopes of mushroom extract was found to be 1.258 mV per decade, in LSV; -assay of <i>Morchella esculenta</i> L. as ethnomedicinal food; -obtained net electrochemical antioxidant power as 2.7 ± 0.12 mg per gram, using ascorbic acid as reference;	[191]
20.	Cyclic voltammetry;	-carbon paste electrode incorporating 2,2-diphenyl-1-picrylhydrazyl;	-supporting electrolyte: Phosphate buffer solution 0.1 M, pH 7.0; -potential ranges investigated: 0.00 V to −1.00 V; 0.60 V to −0.20 V and 0.45 V to 1.10 V, vs. Ag/AgCl; -a peak potential of −833 mV, due to the irreversible reduction of the nitro functions on the phenyl group, present in the structure of DPPH; -for tea extract analyzed, signals recorded in the potential window 0.4 V–1.1 V; -tea extracts presented an anodic peak at about 0.8 V and a cathodic one at around 0.75 V;	[192]
21.	Cyclic voltammetry; Amperometry;	-single walled carbon nanotubes-, graphene- and gold nanoparticles-based screen-printed electrodes;	-supporting electrolyte: Sodium phosphate buffer solution 0.1 M, pH 7.0; -assessment of the quenching capacity of plant extracts (<i>Hippophae fructus</i> and <i>Lavandula Flowers</i>) in the presence of H ₂ O ₂ (chosen as model reactive oxygenated species); -cyclic voltammograms reveal anodic peaks below 0.45 V vs Ag/AgCl, in the presence of extract; -a marked cyclic voltammetric anodic peak at 0.09 V, and a small cathodic peak at 0.35 V noticed for lavender extracts; -amperometric assay based on sensor's sensitivity to H ₂ O ₂ in the absence / presence of the extract; -best sensitivity obtained at the gold nanoparticles-modified sensor: 6.43 ± 0.2 μA cm ⁻² mM ⁻¹ ; -amperometric determinations at constant potential of 0.55 V, with linearity of 2 to 30 mM hydrogen peroxide; -antioxidant capacity determination of hydrosoluble plant extracts;	[17]
22.	Cyclic voltammetry;	-glassy carbon electrode;	-supporting electrolyte: Tetrabutylammonium perchlorate, in dimethyl sulfoxide 99%; -scan rate 25 mV/s in CV; -the voltammograms of the figs and almond extracts presented redox signals at positive potentials, the anodic oxidation being noticed at 1.175 V and 1.218 V, respectively, vs saturated calomel reference; -determination of antioxidant activity of dry fruits (almond, apricot, cashew, figs, peanut, pistachio, raisins, and walnut);	[193]

Table 3. Cont.

No.	Analytical Method	Carbon-Based Working Electrode	Analytical Characteristics	Ref.
23.	Cyclic voltammetry;	-glassy carbon electrode;	<p>-supporting electrolyte: Sodium acetate-acetic acid buffer (0.1 mol L^{-1}, pH = 4.5) in acidified 80% methanol;</p> <p>-analytical cyclic voltammetric signals for all target phenolic compounds present between 0 mV and 800 mV, at a scan rate of 100 mV s^{-1};</p> <p>-cyclic voltammograms of berry fruits presented anodic peaks between 310 mV (quercetin) and 0.756 mV (coumaric acid) vs. Ag/AgCl</p> <p>-antioxidant capacity quantification relied on the area underneath the anodic peak, corresponding to the charge up to a potential value of 500 mV (Q_{500});</p> <p>-evaluation of antioxidant activity of 15 berry samples (strawberries, blackberries, blueberries and red raspberries);</p>	[194]
24.	Amperometry;	-glassy carbon electrode integrated in a flow injection system with sequential diode array and amperometric detection;	<p>-supporting electrolyte: Ethanol 12% v/v and tartaric acid 2 g/L, pH 3.6;</p> <p>-amperometric determinations at 800 mV vs. Ag/AgCl;</p> <p>-calibration curve over the range 0–0.19 mM gallic acid equivalents;</p> <p>-determination of total polyphenol content and antioxidant activity of white, red wines and oenological tannins;</p> <p>-total wine phenolic content between 1.08 and 15.4 mM gallic acid;</p> <p>-concentration range 0.07–0.34 mM gallic acid obtained for tannin solutions;</p>	[195]
25.	Cyclic voltammetry; Differential pulse voltammetry;	-glassy carbon electrode;	<p>-supporting electrolyte: Sodium acetate 0.1 mol L^{-1};</p> <p>-two CV oxidation waves at potentials of 0.45 V and 0.84 V vs Ag/AgCl, pointing towards the presence in the extract of minimum two kinds of reducing species, or a single reducing species that can be oxidized by two stable intermediates;</p> <p>-extracts showed no voltammetric waves in the range of reduction potentials, suggesting that the reducing species in the extract of <i>Mimosa albida</i> leaves can exhibit antioxidant potential;</p> <p>-two oxidation waves noticed on DPVs, indicating the existence of two antioxidant compounds: One species with greater antioxidant capacity with oxidation potential at 0.34 V, and the other one with lower antioxidant power, at 0.79 V;</p> <p>-oxidation signal for <i>Mimosa albida</i>-modified silver nanoparticles at +0.3792 V (CV);</p> <p>-analysis of aqueous leaf extract of <i>Mimosa albida</i> and assay of antioxidant capacity of <i>Mimosa albida</i>-modified silver nanoparticles;</p>	[196]
26.	Differential pulse voltammetry;	-glassy carbon electrode;	<p>-supporting electrolyte: Sodium phosphate buffer solution 0.1 M, pH 7.4;</p> <p>-scan rate 50 mV/s; pulse period 35 ms; potential step 10 mV;</p> <p>-at increasing amounts of added extract, DPV oxidation peaks were noticed, at approximately 0.270 V, 0.430V, and 0.880 V vs. Ag/AgCl;</p> <p>-determination of the antioxidant capacity of the <i>Greigia Sphacelata</i> fruit;</p>	[197]

Table 3. Cont.

No.	Analytical Method	Carbon-Based Working Electrode	Analytical Characteristics	Ref.
27.	Cyclic voltammetry; Differential pulse voltammetry;	-glassy carbon electrodes modified with carbon nanotubes and chitosan;	<ul style="list-style-type: none"> -supporting electrolyte: Britton-Robinson electrolyte buffer, at pH 3.0; -chicoric acid anodic peak at 0.610 ± 0.060 V and cathodic peak at 435 ± 0.055 V vs Ag/AgCl, at 300 mV s^{-1} scan rate; -the intensities of oxidation and reduction currents linearly vary with the square root of the scanning speed, in cyclic voltammetry; -DPVs showed oxidation peaks for caftaric acid at 0.505 ± 0.002 V, and for chicoric acid at 0.515 ± 0.001 V vs Ag/AgCl, which are consistent with the results obtained at the assay of pharmaceutical forms; -determination of total polyphenol content and antioxidant activity of <i>Echinacea purpurea</i> extracts in 3 different pharmaceutical forms (capsules, tablets and tincture); 	[198]
28.	Staircase voltammetry;	glassy carbon electrode;	<ul style="list-style-type: none"> -supporting electrolyte-100 mM KNO_3; -staircase voltammograms recorded successively for 4 cycles between +1.0 and -1.2 V vs Ag/AgCl; -scan rate 50 mV/s, starting and ending in +1.0 V; -the half-wave potential ($E_{1/2}$), or the potential corresponding to half the anodic peak current (I_{pa}) was considered; lower $E_{1/2}$ values are correlated to higher antioxidant potential; -the peak intensity or, more accurately the surface area under the oxidation peak, provided quantitative informations: Antioxidant concentration/antioxidant capacity; -analytical peaks present between -0.6 and 0 V, and around 0.5 V; -evaluation of antioxidant activity for teas, wines and (superfood) juices; -antioxidant index calculated relying on the maximum charge of oxidation (Q_{max}), the standard potential of the oxygen evolution reaction (vs. Ag/AgCl) and the standard potential of hydrogen evolution reaction (vs. Ag/AgCl); 	[199]
29.	Cyclic voltammetry;	-glassy carbon electrode;	<ul style="list-style-type: none"> -supporting electrolyte $-0.1 \text{ M H}_2\text{SO}_4$ solution; -scan rate investigated in the range of 20–160 mV s^{-1}; -dependence of charge under the anodic peak, on the concentration of tested red corn pigments, quantified in the region -0.2–1.2 V; -CV for dark red corn seeds extract (1 mg mL^{-1}) presents two anodic peaks at about 0.4 V and 0.65 V; a cathodic peak at the reverse scan, at about 0.2 V vs saturated calomel reference; -evaluation of total phenolic and flavonoid contents in red corn; 	[200]
30.	Voltammetry;	-carbon fiber ultramicroelectrodes;	<ul style="list-style-type: none"> -linear relationship between anodic peak current and caffeic acid (reference antioxidant) concentration from 3.0 to 500 $\mu\text{mol L}^{-1}$; -repeatability illustrated by a RSD of 2.7%; -sensitivity 12 $\mu\text{A L mol}^{-1}$; -Ag/AgCl electrode used as reference; -LOD 0.41 $\mu\text{mol L}^{-1}$; -LOQ 1.26 $\mu\text{mol L}^{-1}$; -estimation of antioxidant capacity in three different wines, and in green and red grape samples; 	[201]

Table 3. Cont.

No.	Analytical Method	Carbon-Based Working Electrode	Analytical Characteristics	Ref.
31	Cyclic voltammetry; Square-wave voltammetry;	-carbon electrode modified with guanine-, polythionine-, and nitrogen-doped graphene;	-determinations performed in PBS pH = 1.5; -1.0 mg/mL ⁻¹ guanine solution as optimum for modification of the electrode; -a pair of redox peaks found between 0 and 0.3 V in CV; peak currents increased with increasing scan times; a thin blue membrane formed on the surface of electrode, showed that thionine was successfully polymerized; -oxidation peak for ascorbic acid at about 1.1 V (SWV); -linear range for ascorbic acid (standard antioxidant) analytical response ranged from 0.5 to 3.0 mg L ⁻¹ in SWV; -LOD 0.21 mg L ⁻¹ (SWV); -RSD 3.1% (SWV); -determination of antioxidant capacity of fruit juices (grape juice, guava juice, and orange juice) and jute leaves extract, ramie leaves extract, and hemp leaves extract;	[202]
32	Differential pulse stripping voltammetry (DPSV); Cyclic voltammetry;	-glassy carbon electrode modified with polyglycine;	-supporting electrolyte: Britton-Robinson electrolyte buffer, pH 3.0; -well-configured oxidation peak of quercetin (model antioxidant) occurs at around +460 mV, a corresponding cathodic peak being visible at 420 mV vs Ag/AgCl; -peaks shifted towards less positive potentials when the scan rates increased from 20 to 400 mV/s in CV; -oxidation peak current assigned to phenolic compounds of yam, at 430 mV, consistent to the peak potential of quercetin, on differential pulse stripping voltammograms; -DPSV-pulse amplitude of 50 mV, pulse width of 500 ms; -LOD 0.39 µg L ⁻¹ (DPSV); -LOQ 1.39 µg L ⁻¹ (DPSV); -electrode modification resulted in 3.15-fold increase of sensitivity, when compared to the bare glassy carbon; -total antioxidant capacity of 0.1 kg of yam, obtained as 96.15 ± 0.85 µg/L of equivalents quercetin at 95% confidence level; -relative standard deviation of 0.88%;	[203]
33	Cyclic voltammetry; Chronoamperometry;	-biosensor based on laccase immobilized onto a gold nanoparticles/graphene nanoplatelets-modified screen-printed carbon electrode;	-supporting electrolyte: Sodium phosphate buffer solution 0.1M, pH 7.0; -potential range from -0.6 V to 1.2 V with a scan rate of 0.05 V/s and a step potential of 2.0 mV (CV); -anodic and cathodic CV peaks of hydroquinone at 0.2 V vs Ag/AgCl and 0 V, respectively, at a scan rate of 0.05 V s ⁻¹ ; -excellent electrocatalytic activity towards oxidation of hydroquinone at a potential of -0.05 V in hydrodynamic amperometry; -linear range 4–130 µM (chronoamperometry); -LOD 1.5 µM chronoamperometry) -LOQ 5 µM (chronoamperometry); -determination of phenolic antioxidant capacity in wine and blueberry syrup;	[204]

Table 3. Cont.

No.	Analytical Method	Carbon-Based Working Electrode	Analytical Characteristics	Ref.
34.	Cyclic voltammetry;	-glassy carbon electrode;	-supporting electrolyte: 0.1 M sodium acetate/acetic acid bufer solution, pH 3.6; -potential scans performed from -0.4 V to 1 V vs Ag/AgCl at a scan rate of 25 mV s^{-1} ; -total antioxidant capacity expressed as ascorbic acid equivalents; -crude medicinal plant extracts exhibited an oxidation peak around 750 mV on cyclic voltammograms; -medicinal plant extracts have less than 36 times smaller total antioxidant capacity, when compared to ascorbic acid; -it was concluded that cyclic voltammetry and FRAP are recommended for flavonoid quantitation;	[205]

5. Critical Perspectives and Comparative Conclusions

Analytical parameters of carbon-based sensors, analyte oxidation–reduction steps and potentials are influenced by analyte chemical structure (number and position of $-\text{OH}$ groups or other substituents), electrode type, its development and interaction with the antioxidant molecule, as well as working conditions (matrix characteristics such pH or presence of interferences).

Studies performed on ascorbic acid electro-oxidation reveal irreversible voltammograms, consistent with the reported mechanism describing electrochemically reversible electron transfer, and a subsequent irreversible chemical process. During the first step, the oxidation of ascorbic acid involves liberation of two electrons and two protons, yielding dehydroascorbic acid. This electron transfer is followed by an irreversible solvation reaction at $\text{pH} < 4.0$. At pH values smaller than the first pK_a value of L-ascorbic acid (around 4.5), two protons are exchanged during the process, whereas at higher pH values (4.5–8.0), a single proton is released, giving ascorbate anion as electroactive compound [206,207]. These described oxidation/solvation steps are consistent with the variation of the peak potential with pH, noticed up to pH 8.0, at a gold electrode: A pH increase from strong acidic to mild acidic and neutral values, results in anodic peak displacement to more positive values. Reported mechanistic aspects underlying ascorbic acid oxidation at $\text{pH} > 8.0$ imply ascorbate anion oxidation to a diketolactone, which by dehydration gives dehydroascorbic acid, that eventually suffers isomerisation to an ene-diol oxidizable at higher potentials [207].

Studies performed at a glassy carbon electrode modified by single-walled carbon nanotube/zinc oxide, proved that ascorbic acid anodic peak current increased with the increase of pH from 2 to 5, and reached a maximal value for pH comprised between pH 4 and 5. Then, the peak current progressively diminished as the pH increased from 6 to 10 and then increased again, for pH values found between 11 and 12. This confirms the involvement of deprotonation step in the oxidation of ascorbic acid. The oxidation peak shifted towards less positive potential values as the pH increased from 2 to 13. On the irreversible voltammograms obtained at the modified electrode, the oxidation potential shifted by approximately 240 mV towards a lower potential and the peak current doubled, when compared to the bare glassy carbon electrode, confirming electrocatalytic effect in a diffusion-controlled process (linear dependence of the current intensity on the square root of scan rate was observed) [208].

At a p-phenylenediamine film–holes modified glassy carbon electrodes, the cyclic voltammetric oxidation peak current of ascorbic acid increased, as the pH increased from pH 2 to 5. A further pH increase of the buffer resulted in a decrease of the analytical signal. This observation is consistent with the described analyte–electrode interaction: Within the pH range for which the modifier film is positively charged and the analyte is found in

anionic form, the interaction of the modified glassy carbon electrode with ascorbic acid promotes the redox signal. With increasing pH value, the film may adopt a negative charge (caused by adsorption of free OH^-), causing rejection of the anionic form of ascorbic acid. Therefore, the pH value of 5.0 was chosen as optimum, privileging interaction between the cationic film of modifier and the anionic form of analyte [209].

The analysis of anthocyanins by cyclic voltammetry at pH 7.0 revealed for kuromanine (cyanidin-3-O-glucoside) chloride and cyanin (cyanidin-3,5-O-diglucoside) chloride a first reversible peak at around 300 mV, due to the oxidation of catechol moiety present on the B-ring. The oxidized molecule can be subject to further oxidation at higher potential values yielding a second oxidation peak corresponding to the oxidation of the 5,7-dihydroxyl structure of the A-ring (resorcinol moiety). Given the different sensitivities of the techniques, the second peak obtained in cyclic voltammetry is smaller than that obtained in differential pulse voltammetry [129].

Studies on flavonoids reconfirmed first oxidation of the most redox active -OH groups present on ring B. Oxidations of the -OH groups present at C3 on ring C, and on the ring A (in resorcinol group) occur at more positive potentials. Studies on delphinidin anthocyanidin firstly reveal two peaks corresponding to oxidative processes involving -OH groups at 3',4',5' positions (ring B), followed by a third peak corresponding to oxidation of -OH present on position 3 on ring C, and a fourth corresponding to oxidation of -OH groups present at positions 5 and 7 on ring A (resorcinol moiety) [128].

Oxidation of most ortho-diphenols occurs at close potentials, while mono-phenols are oxidized at higher potentials. Phenolic compounds that possess two -OH groups in ortho position on the aromatic ring, are reversibly oxidized to ortho-quinones: They give first peaks appearing on voltammograms, consistent with enhanced electron donating ability typically assigned to catechol-like polyphenols, endowed with highest antioxidant power. Most monophenols are subject to irreversible oxidation, due to only one -OH group. Ortho-diphenols present in olive oil, such as caffeic acid, hydroxytyrosol, and oleuropein are subject to reversible oxidation due to the presence of two hydroxyl groups in ortho position, exhibiting one anodic peak and one corresponding cathodic peak at the reverse scan. Tyrosol was irreversibly oxidized generating one anodic peak, due to the oxidation of only one -OH group present on the benzene ring, with the absence of the corresponding cathodic peak. Ferulic acid, a cinnamic acid derivative presenting only one -OH group, has one oxidation peak, and a much less configured reverse cathodic peak [188].

A cyclic voltammetric study performed on wine phenolics confirmed first oxidation of catechol moieties. Catechol-containing hydroxycinnamic acids, as main phenolics present in white wines exhibit a first peak at around 480 mV, followed by polyphenols with more positive potentials (900–1000 mV) such as coumaric acid and their derivatives. High molecular mass compounds resulting from oxidation of original white wine phenolics during storage can contribute to IInd peak. Catechin-type flavonoids, oligomeric and polymeric tannins present in red wines give a first peak around 440 mV; the second peak at around 680 mV was assigned to malvidin, with slight contribution from other phenolics such as trans-resveratrol; second oxidation of the catechin-type flavonoids resulted in a third anodic peak for red wines at 890 mV [137].

Yakovleva et al. performed an electroactivity-based general classification of the phenolic compounds under study (benzenediols, phenolic acids, flavonoids) into groups: Quercetin, dihydroquercetin, and phenolic acids with two -OH groups at ortho positions (2,3-dihydroxybenzoic, protocatechuic, and caffeic acid) are subject to reversible electro-oxidation at pH 6.0, below 400 mV; polyphenols with -OCH₃ substituents present oxidation peaks in the range 400–600 mV; monophenols such as monohydroxyphenolic acids are oxidized at lower rate, having anodic peak potentials greater than 600 mV; the electron-donating groups -OH, -OCH₃ or -CH₃ present on the aromatic ring, were confirmed to render studied phenols more oxidizable. Monohydroxylated phenolics with methoxy substituents could be faster oxidized by electron donation than monohydroxyphenols lacking methoxy groups. It was stipulated that the mechanism underlying this trend is the

stabilizing effect of the methoxy groups in the phenoxyl radical formed after electron loss by phenolic compounds [136].

In a study focused on the electrochemical behavior of anthocyanins and anthocyanidins, comparing myrtillin chloride (that has a pyrogallol group on the B-ring) with oenin chloride (that has a hydroxyl group on C4', placed in ortho position with respect to two methoxy groups), the methoxy groups could not impart the previously discussed oxidation facility, the reverse effect being noticed: Hydroxyl group from pyrogallol moiety on the B-ring (the case of myrtillin chloride) was oxidized with greater facility than the hydroxyl group placed in the ortho position with respect to two methoxyl groups (the case of oenin chloride). Moreover, the hydroxyl group found in the ortho-position with respect to two methoxyl groups (in oenin chloride), was more oxidizable than the catechol group placed in the ortho position with respect to a single methoxy group (in petunidin chloride) [129].

Electrochemical studies on phenolic antioxidants are performed in acid media or, most of them, close to physiological pH values, to hamper irreversible conversion of polyphenols at alkaline values. Cyclic voltammograms recorded for some phenolic acids and flavones at pH higher than 8.0 were characterized by irreversibility, and the anodic oxidation potential could not be precisely assessed [136]. It was asserted that phenolic acids can suffer dimerization and polymerization, synchronous with their oxidation by one-electron loss [210]. An increase of the pH value was corroborated with a linear diminution of the oxidation potentials in the case of anthocyanins. Moreover, an enhanced adsorption of the oxidation products (with fouling the electrode surface) was also noticed, correlated to a dramatic anthocyanins' oxidation peaks decrease during second scan, at all pH values [129].

During a study performed on major phenolics present in coffee, an inverse linear dependence of oxidation peak potential vs pH was observed until reaching the pKa value, with a slope of approximately 59.2 mV, close to the Nerstian theoretical value, describing an electron:proton transfer processes. On the differential pulse voltammograms obtained for 0.5% w/v coffee sample, highest peak currents were noticed at middle-acid pH values (ranging between 5.0 and 6.0), while the slope was broken and peak currents diminished at alkaline pH of 8.0. The same observation was valid for voltammograms of hydroxycinnamic acid derivatives. It was concluded that the redox behavior of electroactive species from coffee samples is dominated by catechol-like main redox contributors, endowed with most enhanced antioxidant features [177].

A series of electroanalytical methods have proved their viability in antioxidant and antioxidant activity assay, largely employed being cyclic, differential pulse and amperometric techniques. In differential pulse and square wave techniques, the influence of capacitive currents is hampered, promoting sensitivity and detection of irreversible oxidation–reduction processes linked to the presence of minor electroactive contributors. Moreover, linear scan (cyclic voltammetric) techniques proved their viability in the comparative study of antioxidants' electroactivity (relying on peak position), as well as in antioxidant capacity assay (based on the area under the anodic peak).

Carbonaceous electrode properties affecting electrochemical response are represented by surface properties, electronic structure, adsorption, electrocatalytical behavior and surface preparation [211]. The performances of carbon electrodes as working electrodes depend on the structure of the electrode, on the chemical bonds established between the carbon atoms, as these factors influence mechanical, conductive and chemical features. Considering allotropic carbon forms, diamond, whose structure is ensured by sp³ bonds, has poor conductivity, thus requiring boron doping. Carbon allotropic forms whose structure is ensured by sp² bonds are endowed with convenient electrical features, mainly conductivity.

Electrochemical determinations rely on surface phenomena and thus, electrode surface represents an important characteristic influencing analytical performances, reaction kinetics and interactions with the compounds to be analyzed. Electrode surfaces are commonly polished using alumina, mainly in the case of glassy carbon. A significant voltammetric current increase was reported in the case of gallic acid, chlorogenic acid, caffeic acid,

catechin, rutin and quercetin, as consequence of surface modification with alumina, by mere abrasive polishing [98]. It was found that modification of the glassy carbon electrode surface with small amounts of alumina can result in enhanced apparent catalysis of electron transfer involving catechol at low pH value. It was reported that catechol suffers adsorption on alumina, not directly on the electrode, so the process involves the triple boundary present between alumina particles, analyzed solution and the electrode. Enhancement of catechol redox process takes place at low pH, as such values facilitate the proton-coupled electron transfer at the previously-mentioned three-phase boundary [94]. The antioxidant capacity and activity, as well as the electrochemical index are significantly influenced by the presence of alumina in the case of tea, wine and phytotherapeutics samples. The improvement in detectability and sensitivity recommends the use of alumina-modified glassy carbon electrode for this assay. The shift of the anodic peak potentials towards less-positive values was reported, thus indicating that the electron transfer is promoted by surface modified with alumina. Nevertheless, the reported diminution in the difference between peak potentials (affecting peak-to-peak discrimination), may constitute a shortcoming in the case of surface modification with alumina [98].

Glassy carbon electrodes are prone to other modification methods: Electrode coating with ionic polymers was applied due to their ability to enhance conductive properties. A glassy carbon electrode coated with a thin film of poly(trihexylvinylbenzylammonium chloride) proved permselectivity to uric acid, that presented a linear voltammetric analytical response in the concentration range of 1–10 μM [212]. A glassy carbon electrode modified with multi-walled carbon nanotubes dispersed in polyhistidine allowed for simultaneous differential pulse voltammetric determination of ascorbic acid and paracetamol with improved analytical responses at minimized overvoltage and under diffusion control, benefiting from large electroactive area and enhanced electrocatalytic properties [213].

Electrolytes influence the surface of carbonaceous electrodes. Studies performed in sulfuric acid 4.5 M confirmed a change in composition of surface compounds, removal of finely crystalline graphite, as well as of unstable functional groups from the surface of activated carbon [214].

Conventional carbon-based sensors include glassy carbon, carbon fiber or pyrolytic graphite electrodes. Developing sensors at sizes below 100 nm is often a key characteristic that typically results in high surface area and improved surface/volume ratio. Other distinctive, attractive properties are swift electron transfer, enhanced electrocatalytic activity, improved interfacial adsorption and biocompatibility, when compared to other conventional materials [215,216]. Carbon-based nanomaterials composed of graphitic-type atoms linked by sp^2 bonds, include fullerenes, carbon nanotubes and graphene. Their behavior depends on the interactions established with other materials and atomic or molecular structures [215,217–220]. These nanomaterials possess hollow or layered structures, and can establish non-covalent linkages with organic species through π - π stacking, hydrophobic interactions, hydrogen bonding, van der Waals or electrostatic forces [215,221].

Carbon nanomaterials are prone to combination with a series of other nanomaterials (based on noble metal nanocrystals, ceramics or Teflon) giving rise to nanocomposites with improved characteristics in a distinctive, novel material [215]. Previously reported novel application reveals that oxidation peaks of key analytes such as ascorbic acid, dopamine and uric acid at a ZnO nanosheet arrays/graphene foam sensor, are higher than those obtained at metal oxide-based (indium tin oxide) electrode, proving enhanced electrochemical features in the assay of both analytes, linked to the high conductivity of 3D porous graphene foam and large specific surface imparted by ZnO nanosheet arrays [222]. Diminished ascorbic acid overpotential and good peak-to-peak DPV separation for ascorbic acid vs dopamine (218.0 mV), dopamine vs paracetamol (218.0 mV), and ascorbic acid vs paracetamol (436.0 mV) were reported for platinum nanoparticles-decorated graphene nanocomposite electrode, with performances improved versus graphene-modified glassy carbon electrode and bare glassy carbon electrode [125]. A ZnO nanorods/graphene

nanosheets/indium tin oxide hybrid electrode allowed good discrimination between uric acid and ascorbic acid, peaks at ZnO nanorods/indium tin oxide being not configured [150].

Carbon paste electrodes are synthesized by combining carbon-based materials (carbon nanotubes, microspheres or nanofibers, acetylene black, graphite and diamond,) with a binder (silicon oil or mineral oil) and largely used in antioxidant assay. A highly rigorous control over pasting liquid amount is required, as large amounts, although able to lower background currents, may diminish electron transfer rates [223,224]. These materials are easy to synthesize, inexpensive, possess reduced ohmic resistance, have broad potential range. They are prone to facile modification by using redox complexes, metal oxides or ionic surfactants, to improve performances in voltammetric assays [88]. The use of a carbon paste electrode modified with copper oxide-decorated reduced graphene enabled simultaneous voltammetric assay of ascorbic acid, uric acid and cholesterol, with sensitivity and good separation in SWV [127].

Employing printing technologies for rapid assay of electroactive species benefits from adaptability, compactibility, reduced costs, facility of large scale production, onsite application and easy modifier incorporation. Characteristics such as the employed ink material, the type of substrate, the choice of a particular electrochemical technique, the extent of waste generation, the obtained analytical performances, as well as shortcomings of each application of printed electrode should be considered. Researches should be focused on developing printed electrodes characterized by best analytical performances, lacking hazardous effects to the environment, to successfully replace conventional electrochemical cells [225].

The applications of chemical and biochemical carbon-based sensors encompass swift evaluation of key antioxidants and antioxidant activity in foodstuffs and dietary supplements, as well as in various biological media, these aspects being tightly related to screening/maintaining health status, hence the permanent interest in improving analytical performances and adaptability.

Electrode modification with single-, multiwalled carbon nanotubes or noble metal nanoparticles promotes electrocatalytical features, facilitating electron transfer: Peaks appear at lower potential and have higher corresponding current intensity. Hybrid nanosensors made of carbonaceous materials and metal/metal oxides enable for antioxidant signal separation and enhanced sensitivity in complex media.

Author Contributions: Conceptualization, A.M.P.; A.P.; and A.I.S.; validation, F.I.; L.S.; and L.B.; formal analysis, A.M.P.; A.P.; and A.I.S.; investigation, A.M.P.; A.P.; F.I.; L.S.; L.B.; and A.I.S.; writing—original draft preparation A.M.P.; A.P.; and A.I.S.; writing—review and editing, F.I.; L.S.; and L.B.; visualization, F.I.; L.S.; L.B.; supervision, A.M.P. and A.I.S. All authors have read and agreed to the published version of the manuscript.

Funding: This research received no external funding.

Institutional Review Board Statement: Not applicable.

Informed Consent Statement: Not applicable.

Conflicts of Interest: The authors declare no conflict of interest.

References

1. Pisoschi, A.M.; Pop, A. The role of antioxidants in the chemistry of oxidative stress: A Review. *Eur. J. Med. Chem.* **2015**, *97*, 55–74. [[CrossRef](#)]
2. Pisoschi, A.M.; Pop, A.; Cimpeanu, C.; Predoi, G. Antioxidant capacity determination in plants and plant-derived products: A review. *Oxid. Med. Cell. Longev.* **2016**, *36*, 2016. [[CrossRef](#)]
3. Pisoschi, A.M.; Pop, A.; Iordache, F.; Stanca, L.; Predoi, G.; Serban, A.I. Oxidative stress mitigation by antioxidants-an overview on their chemistry and influences on health status. *Eur. J. Med. Chem.* **2021**, *209*, 112891. [[CrossRef](#)]
4. Gulcin, I. Antioxidants and antioxidant methods: An updated overview. *Arch. Toxicol.* **2020**, *94*, 651–715. [[CrossRef](#)] [[PubMed](#)]
5. Yin, H.; Xu, L.; Porter, N.A. Free radical lipid peroxidation: Mechanisms and analysis. *Chem. Rev.* **2011**, *111*, 5944–5972. [[CrossRef](#)] [[PubMed](#)]
6. Noguchi, N.; Watanabe, A.; Shi, H. Diverse functions of antioxidants. *Free Radic. Res.* **2001**, *33*, 809–817. [[CrossRef](#)] [[PubMed](#)]

7. Ighodaro, O.M.; Akinloye, O.A. First line defence antioxidants-superoxide dismutase (SOD), catalase (CAT) and glutathione peroxidase (GPX): Their fundamental role in the entire antioxidant defence grid. *Alexandria J. Med.* **2018**, *54*, 287–293. [[CrossRef](#)]
8. Poljsak, B.; Suput, D.; Milisav, I. Achieving the balance between ROS and antioxidants: When to use the synthetic antioxidants. *Oxid. Med. Cell. Longev.* **2013**, *2013*, 956792. [[CrossRef](#)] [[PubMed](#)]
9. Santos-Sánchez, N.F.; Salas-Coronado, R.; Villanueva-Cañongo, C.; Hernández-Carlos, B. Chapter 2, Antioxidant compounds and their antioxidant mechanism. In *Antioxidants*; Shalaby, E., Ed.; InTech Open: London, UK, 2019. [[CrossRef](#)]
10. Prior, R.L.; Wu, X.; Schaich, K. Standardized methods for the determination of antioxidant capacity and phenolics in foods and dietary supplements. *J. Agric. Food Chem.* **2005**, *253*, 4290–4302. [[CrossRef](#)]
11. Jimenez, A.; Selga, A.; Torres, J.L.; Julia, L. Reducing activity of polyphenols with stable radicals of the TTM series. Electron transfer versus H-abstraction reactions in flavan-3-ols. *Org. Lett.* **2004**, *6*, 4583–4586. [[CrossRef](#)]
12. Campesi, I.; Marino, M.; Cipolletti, M.; Romani, A.; Franconi, F. Put “gender glasses” on the effects of phenolic compounds on cardiovascular function and diseases. *Eur. J. Nutr.* **2018**, *57*, 2677–2691. [[CrossRef](#)] [[PubMed](#)]
13. Pisoschi, A.M.; Pop, A.; Cimpeanu, C.; Turcus, V.; Predoi, G.; Iordache, F. Nanoencapsulation techniques for compounds and products with antioxidant and antimicrobial activity—a critical view. *Eur. J. Med. Chem.* **2018**, *157*, 1326–1345. [[CrossRef](#)] [[PubMed](#)]
14. Caroch, M.; Morales, P.; Ferreira, I.C.F.R. Antioxidants: Reviewing the chemistry, food applications, legislation and role as preservatives. *Trends Food Sci. Technol.* **2018**, *71*, 107–120. [[CrossRef](#)]
15. Bunaciu, A.A.; Danet, A.F.; Fleschin, S.; Aboul-Enein, H.Y. Recent applications for in vitro antioxidant assay. *Crit. Rev. Anal. Chem.* **2016**, *46*, 389–399. [[CrossRef](#)]
16. Apak, R.; Özyürek, M.; Güçlü, K.; Çapanoglu, E. Antioxidant activity/capacity measurement. 1. classification, physicochemical principles, mechanisms, and electron transfer (ET)-based assays. *J. Agric. Food Chem.* **2016**, *64*, 997–1027. [[CrossRef](#)] [[PubMed](#)]
17. David, M.; Serban, A.; Popa, C.V.; Florescu, M. A nanoparticle-based label-free sensor for screening the relative antioxidant capacity of hydrosoluble plant extracts. *Sensors* **2019**, *19*, 590. [[CrossRef](#)] [[PubMed](#)]
18. Brainina, K.; Stozhko, N.; Vidrevich, M. Antioxidants: Terminology, methods, and future considerations. *Antioxidants* **2019**, *8*, 297. [[CrossRef](#)] [[PubMed](#)]
19. Pisoschi, A.M.; Negulescu, G.P. Methods for total antioxidant activity determination: A review. *Biochem. Anal. Biochem.* **2012**, *1*, 106. [[CrossRef](#)]
20. Sadeer, N.B.; Montesano, D.; Albrizio, S.; Zengin, G.; Mahomoodally, M.F. The versatility of antioxidant assays in food science and safety-chemistry, applications, strengths, and limitations. *Antioxidants* **2020**, *9*, 709. [[CrossRef](#)]
21. Romanet, R.; Coelho, C.; Liu, Y.; Bahut, F.; Ballester, J.; Nikolantonaki, M.; Gougeon, R.D. The antioxidant potential of white wines relies on the chemistry of sulfur-containing compounds: An optimized DPPH assay. *Molecules* **2019**, *24*, 1353. [[CrossRef](#)] [[PubMed](#)]
22. Cao, X.; Yang, L.; Xue, Q.; Yao, F.; Sun, J.; Yang, F.; Liu, Y. Antioxidant evaluation-guided chemical profiling and structure-activity analysis of leaf extracts from five trees in *Broussonetia* and *Morus* (Moraceae). *Sci. Rep.* **2020**, *10*, 4808. [[CrossRef](#)] [[PubMed](#)]
23. Ilyasov, I.R.; Beloborodov, V.L.; Selivanova, I.A.; Terekhov, R.P. ABTS/PP decolorization assay of antioxidant capacity reaction pathways. *Int. J. Mol. Sci.* **2020**, *21*, 1131. [[CrossRef](#)] [[PubMed](#)]
24. Turkiewicz, I.P.; Wojdyło, A.; Tkacz, K.; Nowicka, P.; Golis, T.; Bąbelewski, P. ABTS On-Line antioxidant, α -amylase, α -glucosidase, pancreatic lipase, acetyl- and butyrylcholinesterase inhibition activity of chaenomeles fruits determined by polyphenols and other chemical compounds. *Antioxidants* **2020**, *9*, 60. [[CrossRef](#)]
25. Payne, A.C.; Mazzer, A.; Clarkson, G.J.J.; Taylor, G. Antioxidant assays-consistent findings from FRAP and ORAC reveal a negative impact of organic cultivation on antioxidant potential in spinach but not watercress or rocket leaves. *Food Sci. Nutr.* **2013**, *1*, 439–444. [[CrossRef](#)]
26. Chaves, N.; Santiago, A.; Alías, J.C. Quantification of the antioxidant activity of plant extracts: Analysis of sensitivity and hierarchization based on the method used. *Antioxidants* **2020**, *9*, 76. [[CrossRef](#)] [[PubMed](#)]
27. Berker, K.I.; Güçlü, K.; Tor, I.; Demirata, B.; Apak, R. Total antioxidant capacity assay using optimized ferricyanide/prussian blue method. *Food Anal. Methods* **2010**, *3*, 154–168. [[CrossRef](#)]
28. Meng, J.; Fang, Y.; Zhang, A.; Chen, S.; Xu, T.; Ren, Z.; Han, G.; Liu, J.; Li, H.; Zhang, Z.; et al. Phenolic content and antioxidant capacity of Chinese raisins produced in Xinjiang Province. *Food Res. Int.* **2011**, *44*, 2830–2836. [[CrossRef](#)]
29. Özyürek, M.; Güçlü, K.; Tütem, E.; Başkan, K.S.; Erçağ, E.; Çelik, S.E.; Baki, S.; Yıldız, L.; Karamanc, Ş.; Apak, R. A comprehensive review of CUPRAC methodology. *Anal. Methods* **2011**, *11*, 2439–2453. [[CrossRef](#)]
30. Çekiç, S.D.; Demir, A.; Başkan, K.S.; Tütem, E.; Apak, R. Determination of total antioxidant capacity of milk by CUPRAC and ABTS methods with separate characterisation of milk protein fractions. *J. Dairy Res.* **2015**, *82*, 177–184. [[CrossRef](#)]
31. Catalán, V.; Frühbeck, G.; Gómez-Ambrosi, J. Inflammatory and oxidative stress markers in skeletal muscle of obese subjects. In *Oxidative Stress and Dietary Antioxidants*; del Moral, A.M., García, C.M.A., Eds.; Elsevier: Amsterdam, The Netherlands, 2018; pp. 163–189.
32. De Leon, J.A.D.; Borges, C.R. Evaluation of oxidative stress in biological samples using the thiobarbituric acid reactive substances assay. *J. Vis. Exp.* **2020**, *159*, e61122. [[CrossRef](#)]
33. Benbouguerra, N.; Richard, T.; Saucier, C.; Garcia, F. Voltammetric behavior, flavanol and anthocyanin contents, and antioxidant capacity of grape skins and seeds during ripening (*Vitis vinifera* var. Merlot, Tannat, and Syrah). *Antioxidants* **2020**, *9*, 800. [[CrossRef](#)] [[PubMed](#)]

34. Mohtar, L.G.; Messina, G.A.; Bertolino, F.A.; Pereira, S.V.; Raba, J.; Nazareno, M.A. Comparative study of different methodologies for the determination the antioxidant activity of Venezuelan propolis. *Microchem. J.* **2020**, *158*, 105244. [[CrossRef](#)]
35. Roy, M.K.; Koide, M.; Rao, T.P.; Okubo, T.; Ogasawara, Y.; Juneja, L.R. ORAC and DPPH assay comparison to assess antioxidant capacity of tea infusions: Relationship between total polyphenol and individual catechin content. *Int. J. Food Sci. Nutr.* **2010**, *61*, 109–124. [[CrossRef](#)] [[PubMed](#)]
36. Litescu, S.C.; Eremia, S.A.V.; Tache, A.; Vasilescu, I.; Radu, G.-L. The use of Oxygen Radical Absorbance Capacity (ORAC) and Trolox Equivalent Antioxidant Capacity (TEAC) assays in the assessment of beverages' antioxidant properties. In *Processing and Impact on Antioxidants in Beverages*; Preedy, V., Ed.; Elsevier: Amsterdam, The Netherlands, 2014; pp. 245–251.
37. Romero-Diez, R.; Rodriguez-Rojo, S.; Cocero, M.J.; Duarte, C.M.M.; Matias, A.A.; Bronze, M.R. Phenolic characterization of aging wine lees: Correlation with antioxidant activities. *Food Chem.* **2018**, *259*, 188–195. [[CrossRef](#)] [[PubMed](#)]
38. Denev, P.; Todorova, V.; Ognyanov, M.; Georgiev, Y.; Yanakieva, I.; Tringovska, I.; Grozeva, S.; Kostova, D. Phytochemical composition and antioxidant activity of 63 Balkan pepper (*Capsicum annuum* L.) accessions. *J. Food Meas. Charact.* **2019**, *13*, 2510–2520. [[CrossRef](#)]
39. Gupta, D. Methods for determination of antioxidant capacity: A review. *Int. J. Pharm. Sci. Res.* **2015**, *6*, 546–566.
40. Xiao, F.; Xu, T.; Lu, B.; Liu, R. Guidelines for antioxidant assays for food components. *Food Front.* **2020**, *1*, 60–69. [[CrossRef](#)]
41. Tomassetti, M.; Serone, M.; Angeloni, R.; Campanella, L.; Mazzone, E. Amperometric enzyme sensor to check the total antioxidant capacity of several mixed berries. Comparison with two other spectrophotometric and fluorimetric methods. *Sensors* **2015**, *15*, 3435–3452. [[CrossRef](#)] [[PubMed](#)]
42. Tubaro, F.; Pizzuto, R.; Raimo, G.; Paventi, G. A novel fluorimetric method to evaluate red wine antioxidant activity. *Period. Polytech. Chem. Eng.* **2019**, *63*, 57–64. [[CrossRef](#)]
43. Shpigun, L.K.; Arharova, M.A.; Brainina, K.Z.; Ivanova, A.V. Flow injection potentiometric determination of total antioxidant activity of plant extracts. *Anal. Chim. Acta* **2006**, *573–574*, 419–426. [[CrossRef](#)]
44. Brainina, K.Z.; Stozhko, N.Y.; Buharinova, M.A.; Khamzina, E.I.; Vidrevich, M.B. Potentiometric method of plant microsuspensions antioxidant activity determination. *Food Chem.* **2019**, *278*, 653–658. [[CrossRef](#)]
45. Chevion, S.; Roberts, M.A.; Chevion, M. The use of cyclic voltammetry for the evaluation of antioxidant capacity. *Free Radic. Biol. Med.* **2000**, *28*, 860–870. [[CrossRef](#)]
46. Cardenas, A.; Frontana, C. Evaluation of a carbon ink chemically modified electrode incorporating a copper-neocuproine complex for the quantification of antioxidants. *Sens. Actuators B Chem.* **2020**, *313*, 128070. [[CrossRef](#)]
47. Lubeckyj, R.A.; Winkler-Moser, J.K.; Fhaner, M.J. Application of differential pulse voltammetry to determine the efficiency of stripping tocopherols from commercial fish oil. *J. Am. Oil Chem. Soc.* **2017**, *94*, 527–536. [[CrossRef](#)]
48. Trofin, A.E.; Trinca, L.C.; Ungureanu, E.; Ariton, A.M. CUPRAC voltammetric determination of antioxidant capacity in tea samples by using screen-printed microelectrodes. *J. Anal. Methods Chem.* **2019**, *2019*, 8012758. [[CrossRef](#)] [[PubMed](#)]
49. Giovagnoli-Vicuña, C.; Pizarro, S.; Briones-Labarca, V.; Delgadillo, A. A square wave voltammetry study on the antioxidant interaction and effect of extraction method for binary fruit mixture extracts. *J. Chem.* **2019**, *3*, 1–10. [[CrossRef](#)]
50. Savan, E.K. Square wave voltammetric (SWV) determination of quercetin in tea samples at a single-walled carbon nanotube (SWCNT) modified glassy carbon electrode (GCE). *Anal. Lett.* **2020**, *53*, 858–872. [[CrossRef](#)]
51. Gordiienko, A.; Blaheyevskiy, M.; Iurchenko, I. A comparative study of phenolic compound antioxidant activity by the polarography method, using microsomal lipid peroxidation in vitro. *Curr. Issues Pharm. Med. Sci.* **2018**, *31*, 186–189. [[CrossRef](#)]
52. Karaman, M.; Tesanovic, K.; Gorjanovic, S.; Pastor, F.T.; Simonovic, M.; Glumac, M.; Pejin, B. Polarography as a technique of choice for the evaluation of total antioxidant activity: The case study of selected *Coprinus Comatus* extracts and quinic acid, their antidiabetic ingredient. *Nat. Prod. Res.* **2019**, in press. [[CrossRef](#)]
53. Pisoschi, A.M.; Cimpeanu, C.; Predoi, G. Electrochemical methods for total antioxidant capacity and its main contributors determination: A review. *Open Chem.* **2015**, *13*, 824–856. [[CrossRef](#)]
54. Sazhina, N.N. Determination of antioxidant activity of various bioantioxidants and their mixtures by the amperometric method. *Russ. J. Bioorganic Chem.* **2017**, *43*, 771–775. [[CrossRef](#)]
55. Tougas, T.P.; Jannetti, J.M.; Collier, W.G. Theoretical and experimental response of a biampereometric detector for flow injection analysis. *Anal. Chem.* **1985**, *57*, 1377–1381. [[CrossRef](#)]
56. Milardovic, S.; Kerekovic, I.; Rumenjak, V. A flow injection biampereometric method for determination of total antioxidant capacity of alcoholic beverages using bienzymatically produced ABTS+. *Food Chem.* **2007**, *105*, 1688–1694. [[CrossRef](#)]
57. Moldoveanu, S. The utilization of gas chromatography/mass spectrometry in the profiling of several antioxidants in botanicals. In *Advances in Chromatography*; Guo, X., Ed.; InTech Open: London, UK, 2014; Chapter 5. [[CrossRef](#)]
58. Viet, T.D.; Xuan, T.D.; Van, T.M.; Andriana, Y.; Rayee, R.; Tran, H.-D. Comprehensive fractionation of antioxidants and GC-MS and ESI-MS fingerprints of *Celastrus hindsii* leaves. *Medicines* **2019**, *6*, 64. [[CrossRef](#)]
59. Merken, H.M.; Beecher, G.R. Measurement of food flavonoids by High-Performance Liquid Chromatography: A review. *J. Agric. Food Chem.* **2000**, *48*, 577–599. [[CrossRef](#)] [[PubMed](#)]
60. Ran, J.; Sun, H.; Xu, Y.; Wang, T.; Zhao, R. Comparison of antioxidant activities and high-performance liquid chromatography analysis of polyphenol from different apple varieties. *Int. J. Food Prop.* **2016**, *19*, 2396–2407. [[CrossRef](#)]
61. Skorupa, A.; Gierak, A. Detection and visualization methods used in thin-layer chromatography. *JPC J. Planar Chromat.* **2011**, *24*, 274–280. [[CrossRef](#)]

62. Gwatidzo, L.; Dzomba, P.; Mangena, M. TLC separation and antioxidant activity of flavonoids from *Carissa bispinosa*, *Ficus sycomorus*, and *Grewia bicolor* fruits. *Nutrire* **2018**, *43*, 3. [[CrossRef](#)]
63. Della Pelle, F.; Compagnone, D. Nanomaterial-based sensing and biosensing of phenolic compounds and related antioxidant capacity in food. *Sensors* **2018**, *18*, 462. [[CrossRef](#)] [[PubMed](#)]
64. Escarpa, A. Lights and shadows on food microfluidics. *Lab Chip* **2014**, *14*, 3213–3224. [[CrossRef](#)] [[PubMed](#)]
65. Kellner, R.; Mermet, J.M.; Otto, M.; Valcarcel, V.; Widmer, H.M. (Eds.) *Analytical Chemistry. A modern Approach to Analytical Science*; Wiley-VCH: Weinheim, Germany, 2004.
66. Milardovic, S.; Ivekovic, D.; Rumenjak, V.; Grabaric, B.S. Use of DPPH•/DPPH redox couple for biamperometric determination of antioxidant activity. *Electroanalysis* **2005**, *17*, 1847–1853. [[CrossRef](#)]
67. Pisoschi, A.M. Biamperometric applications to antioxidant content and total antioxidant capacity assessment: An editorial. *Biochem. Anal. Biochem.* **2015**, *4*, 218. [[CrossRef](#)]
68. Pisoschi, A.M.; Cheregi, M.C.; Danet, A.F. Total antioxidant capacity of some commercial fruit juices: Electrochemical and spectrophotometrical approaches. *Molecules* **2009**, *14*, 480–493. [[CrossRef](#)]
69. Pisoschi, A.M.; Pop, A.; Gajaila, I.; Iordache, F.; Dobre, R.; Cazimir, I.; Serban, A.I. Analytical methods applied to the assay of sulfur-containing preserving agents. *Microchem. J.* **2020**, *105*, 104681. [[CrossRef](#)]
70. Pisoschi, A.M.; Negulescu, G.P.; Pisoschi, A. Ascorbic acid determination by an amperometric ascorbate oxidase-based biosensor. *Rev. Chim.* **2010**, *61*, 339–344.
71. Pisoschi, A.M. Biosensors as bio-based materials in chemical analysis: A Review. *J. Biobased Mater. Bioenergy* **2013**, *7*, 19–38. [[CrossRef](#)]
72. Lahcen, A.A.; Rauf, S.; Beduk, T.; Durmus, C.; Aljedaibi, A.; Timur, S.; Alshareef, H.N.; Amine, A.; Wolfbeis, O.S.; Salama, K.N. Electrochemical sensors and biosensors using laser-derived graphene: A comprehensive review. *Biosens. Bioelectron.* **2020**, *168*, 112565. [[CrossRef](#)]
73. Kucherenko, I.S.; Soldatkin, O.O.; Dzyadevych, S.V.; Soldatkin, A.P. Electrochemical biosensors based on multienzyme systems: Main groups, advantages and limitations—A review. *Anal. Chim. Acta* **2020**, *1111*, 114–131. [[CrossRef](#)]
74. Sochor, J.; Dobes, J.; Krystofova, O.; Ruttkay-Nedecky, B.; Babula, P.; Pohanka, M.; Jurikova, T.; Zitka, O.; Adam, V.; Klejdus, B.; et al. Electrochemistry as a tool for studying antioxidant properties. *Int. J. Electrochem. Sci.* **2013**, *8*, 8464–8489.
75. Peres, A.M.; Sousa, M.E.B.; Veloso, A.C.A.; Estevinho, L.; Dias, L.G. Electrochemical sensors for assessing antioxidant capacity of bee products. In *Chemistry, Biology and Potential Applications of Honeybee Plant-Derived Products*; Susana, M.C., Artur, M.S.S., Eds.; Bentham Science Publishers: Sharjah, United Arab Emirates, 2016; pp. 196–223.
76. David, M.; Serban, A.; Radulescu, C.; Danet, A.F.; Florescu, M. Bioelectrochemical evaluation of plant extracts and gold nanozyme-based sensors for total antioxidant capacity determination. *Bioelectrochemistry* **2019**, *129*, 124–134. [[CrossRef](#)] [[PubMed](#)]
77. David, M.; Florescu, M.; Bala, C. Biosensors for antioxidants detection: Trends and perspectives. *Biosensors* **2020**, *10*, 112. [[CrossRef](#)]
78. Ye, Y.; Ji, J.; Sun, Z.; Shen, P.; Sun, X. Recent advances in electrochemical biosensors for antioxidant analysis in foodstuff. *Trends Anal. Chem.* **2020**, *122*, 115718. [[CrossRef](#)]
79. Arumugam, R.; Chen, T.-W.; Chen, S.-M.; Rajaji, U.; Chinnapaiyan, S.; Chinnathabmi, S.; Subramanian, B.; Yu, J.; Yu, R. Electrochemical sensors and biosensors for redox analytes implicated in oxidative stress: Review. *Int. J. Electrochem. Sci.* **2020**, *15*, 7064–7081. [[CrossRef](#)]
80. Mello, L.D.; Kubota, L.T. Biosensors as a tool for the antioxidant status evaluation. *Talanta* **2007**, *72*, 335–348. [[CrossRef](#)] [[PubMed](#)]
81. Barroso, M.F.; de-los-Santos-Álvarez, N.; Lobo-Castanón, M.J.; Miranda Ordieres, A.J.; Delerue-Matos, C.; Oliveira, M.B.P.P.; Tunon-Blanco, P. DNA-based biosensor for the electrocatalytic determination of antioxidant capacity in beverages. *Biosens. Bioelectron.* **2011**, *26*, 2396–2401. [[CrossRef](#)] [[PubMed](#)]
82. Bonanni, A.; Campanella, L.; Gatta, T.; Gregori, E.; Tomassetti, M. Evaluation of the antioxidant and prooxidant properties of several commercial dry spices by different analytical methods. *Food Chem.* **2007**, *102*, 751–758. [[CrossRef](#)]
83. Gomes, S.A.; Rebelo, M.J. A new laccase biosensor for polyphenols determination. *Sensors* **2003**, *3*, 166–175. [[CrossRef](#)]
84. Böyükbayram, A.; Kiralp, S.; Toppare, L.; Yağci, Y. Preparation of biosensors by immobilization of polyphenol oxidase in conducting copolymers and their use in determination of phenolic compounds in red wine. *Bioelectrochemistry* **2006**, *69*, 164–171. [[CrossRef](#)]
85. Gil, D.M.A.; Rebelo, M.J.F. Evaluating the antioxidant capacity of wines: A laccase-based biosensor approach. *Eur. Food Res. Technol.* **2010**, *231*, 303–308. [[CrossRef](#)]
86. Raymundo-Pereira, P.A.; Silva, T.A.; Caetano, F.R.; Ribovski, L.; Zapp, E.; Brondani, D.; Bergamini, M.F.; Marcolino, L.H., Jr.; Banks, C.E.; Oliveira, O.N., Jr.; et al. Polyphenol oxidase-based electrochemical biosensors: A review. *Anal. Chim. Acta* **2020**, *1139*, 198–221. [[CrossRef](#)]
87. Uslu, B.; Ozkan, S.A. Electroanalytical application of carbon based electrodes to the pharmaceuticals. *Anal. Lett.* **2007**, *40*, 817–853. [[CrossRef](#)]
88. Vytras, K.; Svancara, I.; Metelka, R. Carbon paste electrodes in electroanalytical chemistry. *J. Serb. Chem. Soc.* **2009**, *74*, 1021–1033. [[CrossRef](#)]
89. Apetrei, C.; Apetrei, I.M.; De Saja, J.A.; Rodriguez-Mendez, M.L. Carbon Paste electrodes made from different carbonaceous materials: Application in the study of antioxidants. *Sensors* **2011**, *11*, 1328–1344. [[CrossRef](#)] [[PubMed](#)]

90. Svancara, I.; Walcarius, A.; Kalcher, K.; Vytřas, K. Carbon paste electrodes in the new millennium. *Cent. Eur. J. Chem.* **2009**, *7*, 598–656. [[CrossRef](#)]
91. Sharma, S. Glassy carbon: A promising material for micro-and nanomanufacturing. *Materials* **2018**, *10*, 1857. [[CrossRef](#)] [[PubMed](#)]
92. Li, Z.; Zhang, J.; Zhou, Y.; Shuang, S.; Dong, C.; Choi, M.M.F. Electrodeposition of palladium nanoparticles on fullerene modified glassy carbon electrode for methane sensing. *Electrochim. Acta.* **2012**, *76*, 288–291. [[CrossRef](#)]
93. Aziz, M.A.; Almadi, R.; Yamani, Z.H. Indium tin oxide nanoparticle-modified glassy carbon electrode for electrochemical sulfide detection in alcoholic medium. *Anal. Sci.* **2018**, *34*, 599–604. [[CrossRef](#)]
94. Lin, Q.; Batchelor-McAuley, C.; Compton, R.C. Two-electron, two-proton oxidation of catechol: Kinetics and apparent catalysis. *J. Phys. Chem. C.* **2015**, *119*, 1489–1495. [[CrossRef](#)]
95. Thirumalraj, B.; Palanisamy, S.; Chen, S.M.; Kannan, R.S. Alumina polished glassy carbon electrode as a simple electrode for lower potential electrochemical detection of dopamine in its sub-micromolar level. *Electroanalysis* **2016**, *28*, 425–430. [[CrossRef](#)]
96. Lima, A.P.; Almeida, P.L.; Sousa, R.M.; Richter, E.M.; Nossol, E.; Munoz, R.A.A. Effect of alumina supported on glassy-carbon electrode on the electrochemical reduction of 2, 4, 6-trinitrotoluene: A simple strategy for its selective detection. *J. Electroanal. Chem.* **2019**, *851*, 113385. [[CrossRef](#)]
97. Lima, A.P.; Souza, R.C.; Silva, M.N.T.; Gonçalves, R.F.; Nossol, E.; Richter, E.M.; Lima, R.C.; Munoz, R.A.A. Influence of Al₂O₃ nanoparticles structure immobilized upon glassy-carbon electrode on the electrocatalytic oxidation of phenolic compounds. *Sens. Actuators B Chem.* **2018**, *262*, 646–654. [[CrossRef](#)]
98. Lima, A.P.; dos Santos, W.T.P.; Nossol, E.; Richter, E.M.; Munoz, R.A.A. Critical evaluation of voltammetric techniques for antioxidant capacity and activity: Presence of alumina on glassy-carbon electrodes alters the results. *Electrochim. Acta.* **2020**, *358*, 136925. [[CrossRef](#)]
99. Walcarius, A. Analytical applications of silica-modified electrodes-A comprehensive review. *Electroanalysis* **1998**, *10*, 1217–1235. [[CrossRef](#)]
100. Kholmanov, I.; Cavaliere, E.; Fanetti, M.; Cepek, C.; Gavioli, L. Growth of curved graphene sheets on graphite by chemical vapor deposition. *Phys. Rev. B* **2009**, *79*, 233403–233406. [[CrossRef](#)]
101. Wang, Y.X.; Yang, Z.D.; Gao, L.J. Theoretical study of electronic properties of phenyl covalent functional carbon nanotubes. *J. Mol. Sci.* **2016**, *32*, 259–264.
102. Rao, C.N.R.; Sood, A.K.; Subrahmanyam, K.S.; Govindaraj, A. Graphene: The new two-dimensional nanomaterial. *Angew. Chem. Int. Ed.* **2009**, *48*, 7752–7777. [[CrossRef](#)] [[PubMed](#)]
103. Wang, D.W.; Li, F.; Liu, M.; Lu, G.Q.; Cheng, H.M. 3D aperiodic hierarchical porous graphitic carbon material for high-rate electrochemical capacitive energy storage. *Angew. Chem. Int. Ed.* **2008**, *47*, 373–376. [[CrossRef](#)]
104. Lee, J.; Kim, J.; Hyeon, T. Recent progress in the synthesis of porous carbon materials. *Adv. Mater.* **2006**, *18*, 2073–2094. [[CrossRef](#)]
105. Huang, W.; Zhang, H.; Huang, Y.; Wang, W.; Wei, S. Hierarchical porous carbon obtained from animal bone and evaluation in electric double-layer capacitors. *Carbon* **2011**, *49*, 838–843. [[CrossRef](#)]
106. Hei, Y.; Li, X.; Zhou, X.; Liu, J.; Sun, M.; Sha, T.; Xu, C.; Xue, W.; Bo, X.; Zhou, M. Electrochemical sensing platform based on kelp-derived hierarchical meso-macroporous carbons. *Anal. Chim. Acta.* **2018**, *1003*, 16–25. [[CrossRef](#)] [[PubMed](#)]
107. Wang, J. Carbon-nanotube based electrochemical biosensors: A review. *Electroanalysis* **2005**, *17*, 7–14. [[CrossRef](#)]
108. Sun, N.; Guan, L.; Shi, Z.; Zhu, Z.; Li, N.; Li, M.; Gu, Z. Electrochemistry of fullerene peapod modified electrodes. *Electrochem. Commun.* **2005**, *7*, 1148–1152. [[CrossRef](#)]
109. Bhavani, K.S.; Anusha, T.; Brahman, P.K. Fabrication and characterization of gold nanoparticles and fullerene-C60 nanocomposite film at glassy carbon electrode as potential electro-catalyst towards the methanol oxidation. *Internat. J. Hydrog. Energy* **2019**, *44*, 25863–25873. [[CrossRef](#)]
110. Wissler, M. Graphite and carbon powders for electrochemical applications. *J. Power Sources* **2006**, *156*, 142–150. [[CrossRef](#)]
111. de Oliveira, A.C.; dos Santos, S.X.; Cavalheiro, E.T.G. Graphite-silicone rubber composite electrode: Preparation and possibilities of analytical application. *Talanta* **2008**, *74*, 1043–1049. [[CrossRef](#)] [[PubMed](#)]
112. Noked, M.; Soffer, A.; Aurbach, D. The electrochemistry of activated carbonaceous materials: Past, present, and future. *J. Solid State Electrochem.* **2011**, *15*, 1563–1578. [[CrossRef](#)]
113. Krivenko, A.G.; Manzhos, R.A.; Komarova, N.S.; Kotkin, A.S.; Kabachov, E.N.; Shulga, Z.M. Comparative study of graphite and the products of its electrochemical exfoliation. *Russ. J. Electrochem.* **2018**, *54*, 825–834. [[CrossRef](#)]
114. Karunadasa, K.S.P.; Manoratne, C.H.; Pitawala, H.M.T.G.A.; Rajapakse, R.M.G.A. potential working electrode based on graphite and montmorillonite for electrochemical applications in both aqueous and molten salt electrolytes. *Electrochem Commun.* **2019**, *108*, 106562. [[CrossRef](#)]
115. Pleskov, Y.V. Electrochemistry of diamond: A Review. *Russ. J. Electrochem.* **2002**, *38*, 1275–1291. [[CrossRef](#)]
116. Einaga, Y. Development of electrochemical applications of boron-doped diamond electrodes. *Bull. Chem. Soc. Jpn.* **2018**, *91*, 1752–1762. [[CrossRef](#)]
117. Fan, B.; Rusinek, C.A.; Thompson, C.H.; Setien, M.; Guo, Y.; Rechenberg, R.; Gong, Y.; Weber, A.J.; Becker, M.F.; Purcell, E.; et al. Flexible, diamond-based microelectrodes fabricated using the diamond growth side for neural sensing. *Microsyst. Nanoeng.* **2020**, *6*, 42. [[CrossRef](#)] [[PubMed](#)]
118. Matemadombo, F.; Apetrei, C.; Nyokong, T.; Rodríguez-Méndez, M.L.; de Saja, J.A. Comparison of carbon screen-printed and disk electrodes in the detection of antioxidants using CoPc derivatives. *Sens. Actuators B Chem.* **2012**, *166–167*, 457–466. [[CrossRef](#)]

119. Bordonaba, J.G.; Terry, L.A. Electrochemical behaviour of polyphenol rich fruit juices using disposable screen-printed carbon electrodes: Towards a rapid sensor for antioxidant capacity and individual antioxidants. *Talanta* **2012**, *90*, 38–45. [[CrossRef](#)] [[PubMed](#)]
120. Taleat, Z.; Khoshroo, A.; Mazloum-Ardakan, M. Screen-printed electrodes for biosensing: A review (2008–2013). *Microchim. Acta* **2014**, *181*, 865–891. [[CrossRef](#)]
121. Nesakumar, N.; Berchmans, S.; Alwarappan, S. Chemically modified carbon based electrodes for the detection of reduced glutathione. *Sens. Actuators B Chem.* **2018**, *264*, 448–466. [[CrossRef](#)]
122. Panizza, M.; Cerisola, G. Electrochemical degradation of gallic acid on a BDD anode. *Chemosphere* **2009**, *77*, 1060–1064. [[CrossRef](#)]
123. Pisoschi, A.M.; Pop, A.; Negulescu, G.P.; Pisoschi, A. Determination of ascorbic acid content of some fruit juices and wine by voltammetry performed at Pt and Carbon Paste electrodes. *Molecules* **2011**, *16*, 1349–1365. [[CrossRef](#)] [[PubMed](#)]
124. Badea, M.; Chiperea, S.; Bălan, M.; Floroian, L.; Restani, P.; Marty, J.-L.; Iovan, C.; Țiț, D.M.; Bungău, S.; Taus, N. New approaches for electrochemical detection of ascorbic acid. *Farmacia* **2018**, *66*, 83–87.
125. Kumar, M.A.; Lakshminarayanan, V.; Ramamurthy, S.S. Platinum nanoparticles-decorated graphene-modified glassy carbon electrode toward the electrochemical determination of ascorbic acid, dopamine, and paracetamol. *Comptes Rendus Chim.* **2019**, *22*, 58–72. [[CrossRef](#)]
126. Brainina, Z.K.; Bukharinova, M.A.; Stozhko, N.Y.; Sokolkov, S.V.; Tarasov, A.V.; Vidrevich, M.B. Electrochemical sensor based on a carbon veil modified by phytosynthesized gold nanoparticles for determination of ascorbic acid. *Sensors* **2020**, *20*, 1800. [[CrossRef](#)]
127. Karimi-Maleh, H.; Arotiba, O.A. Simultaneous determination of cholesterol, ascorbic acid and uric acid as three essential biological compounds at a carbon paste electrode modified with copper oxide decorated reduced graphene oxide nanocomposite and ionic liquid. *J. Colloid. Interface Sci.* **2020**, *560*, 208–212. [[CrossRef](#)] [[PubMed](#)]
128. de Lima, A.A.; Sussuchi, E.M.; De Giovani, W.F. Electrochemical and antioxidant properties of anthocyanins and anthocyanidins. *Croat. Chem. Acta* **2007**, *80*, 29–34.
129. Janeiro, P.; Brett, A.M.O. Redox behavior of anthocyanins present in *Vitis vinifera* L. *Electroanalysis* **2007**, *19*, 1779–1786. [[CrossRef](#)]
130. Aguirre, M.J.; Chen, Y.Y.; Isaacs, M.; Matsuhira, B.; Mendoza, L.; Torres, S. Electrochemical behaviour and antioxidant capacity of anthocyanins from Chilean red wine, grape and raspberry. *Food Chem.* **2010**, *121*, 44–48. [[CrossRef](#)]
131. Newair, E.F.; Kilmartin, P.A.; Garcia, F. Square wave voltammetric analysis of polyphenol content and antioxidant capacity of red wines using glassy carbon and disposable carbon nanotubes modified screen-printed electrodes. *Eur. Food Res. Technol.* **2018**, *244*, 1225–1237. [[CrossRef](#)]
132. Ziyatdinova, G.; Ziganshina, E.; Budnikov, H. Voltammetric determination of β -carotene in raw vegetables and berries in Triton X100 media. *Talanta* **2012**, *99*, 1024–1029. [[CrossRef](#)]
133. Čižmek, L.; Komorsky-Lovrić, S. Study of electrochemical behaviour of carotenoids in aqueous media. *Electroanalysis* **2019**, *31*, 83–89. [[CrossRef](#)]
134. Stefan-van Staden, R.I.; Moscalu-Lungu, A.; van Staden, J.F. Determination of β -carotene in soft drinks using a stochastic sensor based on a graphene-porphyrin composite. *Electrochem. Commun.* **2019**, *109*, 106581. [[CrossRef](#)]
135. Čižmek, L.; Komorsky-Lovrić, S. Electrochemistry as a screening method in determination of carotenoids in crustacean samples used in everyday diet. *Food Chem.* **2020**, *309*, 125706. [[CrossRef](#)]
136. Yakovleva, K.E.; Kurzeev, S.A.; Stepanova, E.V.; Fedorova, T.V.; Kuznetsov, B.A.; Koroleva, O.V. Characterization of plant phenolic compounds by cyclic voltammetry. *Appl. Biochem. Microbiol.* **2007**, *43*, 661–668. [[CrossRef](#)]
137. Makhotkina, O.; Kilmartin, P.A. The use of cyclic voltammetry for wine analysis: Determination of polyphenols and free sulfur dioxide. *Anal. Chim. Acta* **2010**, *668*, 155–165. [[CrossRef](#)]
138. Bisetty, K.; Sabela, M.I.; Khulu, S.; Xhakaza, M.; Ramsarup, L. Multivariate optimization of voltammetric parameters for the determination of total polyphenolic content in wine samples using an immobilized biosensor. *Int. J. Electrochem. Sci.* **2011**, *6*, 3631–3643.
139. Robledo, S.N.; Zchetti, V.G.L.; Zon, M.A.; Fernández, H. Quantitative determination of tocopherols in edible vegetable oils using electrochemical ultra-microsensors combined with chemometric tools. *Anal. Chim. Acta* **2013**, *116*, 964–971. [[CrossRef](#)]
140. Malyszko, J.; Karbarz, M. Electrochemical oxidation of trolox and α -tocopherol in acetic acid: A comparative study. *J. Electroanal. Chem.* **2006**, *595*, 136–144. [[CrossRef](#)]
141. Kuraya, E.; Nagatomo, S.; Sakata, K.; Kato, D.; Niwa, O.; Nishimi, T.; Kunitake, M. Simultaneous electrochemical analysis of hydrophilic and lipophilic antioxidants in bicontinuous microemulsion. *Anal. Chem.* **2015**, *87*, 1489–1493. [[CrossRef](#)] [[PubMed](#)]
142. Sys, M.; Švecová, B.; Švancara, I.; Metelka, R. Determination of vitamin E in margarines and edible oils using square wave anodic stripping voltammetry with a glassy carbon paste electrode. *Food. Chem.* **2017**, *229*, 621–627. [[CrossRef](#)]
143. Doblhoff-Dier, O.; Rechnitz, G.A. Amperometric method for the determination of superoxide dismutase activity at physiological pH. *Anal. Chim. Acta* **1989**, *222*, 247–252. [[CrossRef](#)]
144. Santharaman, P.; Das, M.; Singh, S.K.; Sethy, N.K.; Bhargava, K.; Claussen, J.C.; Karunakaran, C. Label-free electrochemical immunosensor for the rapid and sensitive detection of the oxidative stress marker superoxide dismutase 1 at the point-of-care. *Sens. Actuators B Chem.* **2016**, *236*, 546–553. [[CrossRef](#)]
145. Wang, J.; Jiang, Z.; Xie, L.; Liu, M.; Yuan, Z. Determination of the activity of superoxide dismutase using a glassy carbon electrode modified with ferrocene imidazolium salts and hydroxy-functionalized graphene. *Microchim. Acta* **2017**, *184*, 289–296. [[CrossRef](#)]

146. Liu, Q.; Bao, J.; Yang, M.; Wang, X.; Lan, S.; Hou, C.; Wang, Y.; Fa, H. A core-shell MWCNT@rGONR heterostructure modified glassy carbon electrode for ultrasensitive electrochemical detection of glutathione. *Sens. Actuators B Chem.* **2018**, *274*, 433–440. [[CrossRef](#)]
147. De Almeida Ferraza, N.V.; Vasconcelos, W.S.; Silva, C.S.; Alves Junior, S.; Amorim, C.G.; da Conceição Branco, S.M.; Montenegro, M.; Cunha Areias, M.C. Gold-copper metal-organic framework nanocomposite as a glassy carbon electrode modifier for the voltammetric detection of glutathione in commercial dietary supplements. *Sens. Actuators B Chem.* **2020**, *307*, 127636. [[CrossRef](#)]
148. Stojanović, Z.S.; Đurović, A.D.; Ashrafi, A.M.; Koudelková, Z.; Zítka, O.; Richtera, L. Highly sensitive simultaneous electrochemical determination of reduced and oxidized glutathione in urine samples using antimony trioxide modified carbon paste electrode. *Sens. Actuators B Chem.* **2020**, *318*, 128141. [[CrossRef](#)]
149. Das, S.C.; Pandey, R.R.; Devkota, T.; Chusuei, C.C. Raman spectroscopy as an assay to disentangle zinc oxide carbon nanotube composites for optimized uric acid detection. *Chemosensors* **2018**, *6*, 65. [[CrossRef](#)]
150. Wang, Q.; Yue, H.; Zhang, J.; Gao, X.; Zhang, H.; Lin, X.; Wang, B.; Bychanok, D. Electrochemical determination of uric acid in the presence of ascorbic acid by hybrid of ZnO nanorods and graphene nanosheets. *Ionics* **2018**, *24*, 2499–2507. [[CrossRef](#)]
151. Fukuda, T.; Muguruma, H.; Iwasa, H.; Tanaka, T.; Hiratsuka, A.; Shimizu, T.; Tsuji, K.; Kishimoto, T. Electrochemical determination of uric acid in urine and serum with uricase/carbon nanotube /carboxymethylcellulose electrode. *Anal. Biochem.* **2020**, *590*, 113533. [[CrossRef](#)] [[PubMed](#)]
152. Thangamuthu, M.; Gabriel, W.E.; Santschi, C.; Martin, O.J.F. Electrochemical sensor for bilirubin detection using screen printed electrodes functionalized with carbon nanotubes and graphene. *Sensors* **2018**, *18*, 800. [[CrossRef](#)] [[PubMed](#)]
153. Raveendran, J.; Stanley, J.; Sathesh Babu, T.G. Voltammetric determination of bilirubin on disposable screen printed carbon electrode. *J. Electroanal. Chem.* **2018**, *818*, 124–130. [[CrossRef](#)]
154. Akhoundian, M.; Alizadeh, T.; Pan, G. Investigation of electrochemical behavior of bilirubin at unmodified carbon paste electrode. *Anal. Bioanal. Electrochem.* **2019**, *9*, 1166–1175.
155. Apetrei, I.M.; Apetrei, C. Voltammetric determination of melatonin using a graphene-based sensor in pharmaceutical products. *Int. J. Nanomed.* **2016**, *11*, 1859–1866. [[CrossRef](#)]
156. Kumar, N.; Goyal, R.N. Electrochemical behavior of melatonin and its sensing in pharmaceutical formulations and in human urine. *Curr. Pharm. Anal.* **2017**, *13*, 85–90. [[CrossRef](#)]
157. Castagnola, E.; Woepfel, K.; Golabchi, A.; McGuier, M.; Chodapaneedi, N.; Metro, J.; Taylor, I.M.; Tracy Cui, X. Electrochemical detection of exogenously administered melatonin in the brain. *Analyst* **2020**, *145*, 2612–2620. [[CrossRef](#)] [[PubMed](#)]
158. Michalkiewicz, S. Voltammetric determination of coenzyme Q10 in pharmaceutical dosage forms. *Bioelectrochemistry* **2008**, *73*, 30–36. [[CrossRef](#)] [[PubMed](#)]
159. Petrova, E.V.; Korotkova, E.I.; Kratochvil, B.; Voronova, O.A.; Dorozhko, E.V.; Bulycheva, E.V. Investigation of Coenzyme Q10 by voltammetry. *Procedia Chem.* **2014**, *10*, 173–178. [[CrossRef](#)]
160. Charoenkitamorn, K.; Chaiyo, S.; Chailapakul, O.; Siangproh, W. Low-cost and disposable sensors for the simultaneous determination of coenzyme Q₁₀ and α -lipoic acid using manganese (IV) oxide-modified screen-printed graphene electrodes. *Anal. Chim. Acta* **2018**, *1004*, 22–31. [[CrossRef](#)] [[PubMed](#)]
161. Cincotto, F.H.; Canevari, T.C.; Machado, S.A.S. Highly sensitive electrochemical sensor for determination of Vitamin D in mixtures of water-ethanol. *Electroanalysis* **2014**, *26*, 2783–2788. [[CrossRef](#)]
162. Men, K.; Chen, Y.; Liu, J.B.; Wei, D.J. Electrochemical detection of Vitamin D2 and D3 based on a Au-Pd modified glassy carbon electrode. *Int. J. Electrochem. Sci.* **2017**, *12*, 9555–9564. [[CrossRef](#)]
163. Durovic, A.; Stojanovic, Z.; Kravic, S.; Kos, J.; Richtera, L. Electrochemical determination of Vitamin D3 in pharmaceutical products by using boron doped diamond electrode. *Electroanalysis* **2020**, *32*, 741–748. [[CrossRef](#)]
164. Ferreira, A.P.M.; Dos Santos Pereira, L.N.; Santos da Silva, I.; Tanaka, S.M.C.N.; Tanaka, A.A.; Angnes, L. Determination of α -lipoic acid on a pyrolytic graphite electrode modified with cobalt phthalocyanine. *Electroanalysis* **2014**, *26*, 2138–2144. [[CrossRef](#)]
165. Dos Santos Pereira, L.N.; da Silva, I.S.; Araújo, T.P.; Tanaka, A.A.; Angnes, L. Fast quantification of α -lipoic acid in biological samples and dietary supplements using batch injection analysis with amperometric detection. *Talanta* **2016**, *154*, 249–254. [[CrossRef](#)]
166. Ziyatdinova, G.; Antonova, T.; Vorobev, V.; Osin, Y.; Budnikov, H. Selective voltammetric determination of α -lipoic acid on the electrode modified with SnO₂ nanoparticles and cetyltriphenylphosphonium bromide. *Monatsh. Chem.* **2019**, *150*, 401–410. [[CrossRef](#)]
167. Nunes Angelis, P.; de Cássia Mendonça, J.; Rianne da Rocha, L.; Boareto Capelari, T.; Carolyne Prete, M.; Gava Segatelli, M.; Borsato, D.; Ricardo Teixeira Tarley, C. Feasibility of a nano-carbon black paste electrode for simultaneous voltammetric determination of antioxidants in food samples and biodiesel in the presence of surfactant. *Electroanalysis* **2020**, *32*, 1198–1207. [[CrossRef](#)]
168. Pisoschi, A.M.; Pop, A. Comparative sulfite assay by voltammetry using Pt electrodes, photometry and titrimetry: Application to cider, vinegar and sugar analysis. *Open Chem.* **2018**, *16*, 1248–1256. [[CrossRef](#)]
169. Dar, R.A.; Brahman, P.K.; Khurana, N.; Wagay, J.A.; Lone, Z.A.; Ganaie, M.A.; Pitre, K.S. Evaluation of antioxidant activity of crocin, podophyllotoxin and kaempferol by chemical, biochemical and electrochemical assays. *Arab. J. Chem.* **2017**, *10*, S1119–S1128. [[CrossRef](#)]
170. Korotkova, E.I.; Lipskikh, O.I.; Kiseleva, M.A.; Ivanov, V.V. Voltammetric study of the antioxidant properties of catalase and superoxide dismutase. *Pharm. Chem. J.* **2008**, *42*, 485–487. [[CrossRef](#)]

171. Wei, Y.; Zhang, S. Study on the electroreduction process of oxygen to superoxide ion by using acetylene black powder microelectrode. *Russ. J. Electrochem.* **2008**, *44*, 967–971. [[CrossRef](#)]
172. Blasco, A.J.; Rogerio, M.C.; Gonzalez, M.C.; Escarpa, A. “Electrochemical Index” as a screening method to determine “total polyphenolics” in foods: A proposal. *Anal. Chim. Acta* **2005**, *539*, 237–244. [[CrossRef](#)]
173. Abdel-Hamid, R.; Newair, E.F. Voltammetric determination of polyphenolic content in pomegranate juice using a poly(gallic acid)/multiwalled carbon nanotube modified electrode. *Beilstein J. Nanotechnol.* **2016**, *7*, 1104–1112. [[CrossRef](#)]
174. Raymundo-Pereira, P.A.; Campos, A.M.; Prado, T.M.; Furini, L.N.; Boas, N.V.; Calegari, M.L.; Machado, S.A.S. Synergy between Printex nano-carbons and silver nanoparticles for sensitive estimation of antioxidant activity. *Anal. Chim. Acta* **2016**, *926*, 88–98. [[CrossRef](#)]
175. Eguílaz, M.; Gutierrez, A.; Gutierrez, F.; Gonzalez-Domínguez, J.M.; Anson-Casaos, A.; Hernandez-Ferrer, J.; Ferreyra, N.F.; Martínez, M.T.; Rivas, G. Covalent functionalization of single-walled carbon nanotubes with polytyrosine: Characterization and analytical applications for the sensitive quantification of polyphenols. *Anal. Chim. Acta* **2016**, *909*, 51–59. [[CrossRef](#)]
176. Yuan, Y.; Bao, Z.H.; Li, S.M.; Zhao, K. Electrochemical evaluation of antioxidant capacity in pharmaceutical antioxidant excipient of drugs on guanine-based modified electrode. *J. Electroanal. Chem.* **2016**, *772*, 58–65.
177. Oliveira-Neto, J.R.; Garcia Rezende, S.; de Fátima Reis, C.; Rathinaraj Benjamin, S.; Lavorenti Rocha, M.; de Souza Gil, E. Electrochemical behavior and determination of major phenolic antioxidants in selected coffee samples. *Food Chem.* **2016**, *190*, 506–512. [[CrossRef](#)]
178. Tirawattanakoson, R.; Rattanasat, P.; Ngamrojanavanich, N.; Rodthongkum, N.; Chailapakul, O. Free radical scavenger screening of total antioxidant capacity in herb and beverage using graphene/PEDOT: PSS-modified electrochemical sensor. *J. Electroanal. Chem.* **2016**, *767*, 68–75. [[CrossRef](#)]
179. Ziyatdinova, G.; Kozlova, E.; Budnikov, H. Chronocoulometry of wine on multi-walled carbon nanotube modified electrode: Antioxidant capacity assay. *Food. Chem.* **2016**, *196*, 405–410. [[CrossRef](#)] [[PubMed](#)]
180. De Oliveira Neto, J.R.; Rezende, S.G.; Lobón, G.S.; Garcia, T.A.; Macedo, I.Y.L.; Garcia, L.F.; Alves, V.F.; Sapateiro Torres, I.M.; Santiago, M.F.; Schmidt, F.; et al. Electroanalysis and laccase-based biosensor on the determination of phenolic content and antioxidant power of honey samples. *Food Chem.* **2017**, *237*, 1118–1123. [[CrossRef](#)]
181. Della Pelle, F.; Di Battista, R.; Vázquez, L.; Palomares, F.J.; Del Carlo, M.; Sergi, M.; Compagnone, D.; Escarpa, A. Press-transferred carbon black nanoparticles for class-selective antioxidant electrochemical detection. *Appl. Mater. Today* **2017**, *9*, 29–36. [[CrossRef](#)]
182. de Menezes Peixoto, C.R.; Fraga, S.; Justim, J.D.; Gomes, M.S.; Carvalho, D.G.; Jarenkow, J.A.; de Moura, N.F. Voltammetric determination of total antioxidant capacity of *Bunchosia glandulifera* tree extracts. *J. Electroanal. Chem.* **2017**, *799*, 519–524. [[CrossRef](#)]
183. Ziyatdinova, G.K.; Kozlova, E.V.; Budnikov, H.C. Chronoamperometric evaluation of the antioxidant capacity of tea on a polyquercetin-modified electrode. *J. Anal. Chem.* **2017**, *72*, 382–389. [[CrossRef](#)]
184. Jara-Palacios, M.J.; Escudero-Gilete, M.L.; Hernández-Hierro, J.M.; Heredia, F.J.; Hernanz, D. Cyclic voltammetry to evaluate the antioxidant potential in winemaking by-products. *Talanta* **2017**, *165*, 211–215. [[CrossRef](#)]
185. Samoticha, J.; Jara-Palacios, M.J.; Hernández-Hierro, J.M.; Heredia, F.J.; Wojdyło, A. Phenolic compounds and antioxidant activity of twelve grape cultivars measured by chemical and electrochemical methods. *Eur. Food Res. Technol.* **2018**, *244*, 1933–1943. [[CrossRef](#)]
186. De Siqueira Leite, K.C.; Garcia, L.F.; Lobón, G.S.; Thomaz, D.V.; Goncalves Moreno, E.K.; de Carvalho, M.F.; Rocha, M.L.; dos Santos, W.T.P.; de Souza Gil, E. Antioxidant activity evaluation of dried herbal extracts: An electroanalytical approach. *Rev. Bras. Farmacogn.* **2018**, *28*, 325–332. [[CrossRef](#)]
187. Lugonja, N.M.; Stanković, D.M.; Miličić, B.; Spasić, S.D.; Marinković, V.; Vrvic, M.M. Electrochemical monitoring of the breast milk quality. *Food Chem.* **2018**, *240*, 567–572. [[CrossRef](#)]
188. Fernández, E.; Vidal, L.; Canals, A. Rapid determination of hydrophilic phenols in olive oil by vortex-assisted reversed-phase dispersive liquid-liquid microextraction and screen-printed carbon electrodes. *Talanta* **2018**, *181*, 44–51. [[CrossRef](#)] [[PubMed](#)]
189. David, I.G.; Litescu, S.C.; Popa, D.E.; Buleandra, M.; Iordache, L.; Albu, C.; Alecu, A.; Penu, R.L. Voltammetric analysis of naringenin at a disposable pencil graphite electrode-application to polyphenol content determination in citrus juice. *Anal. Methods* **2018**, *10*, 5763–5772. [[CrossRef](#)]
190. Arantes, I.V.S.; Stefano, J.S.; Sousa, R.M.F.; Richter, E.M.; Foster, C.W.; Banks, C.E.; Munoz, R.A.A. Fast determination of antioxidant capacity of food samples using continuous amperometric detection on polyester screen-printed graphitic electrodes. *Electroanalysis* **2018**, *30*, 1192–1197. [[CrossRef](#)]
191. Wagay, J.A.; Nayik, G.A.; Wani, S.A.; Mir, R.A.; Ahmad, M.A.; Rahman, Q.I.; Vyas, D. Phenolic profiling and antioxidant capacity of *Morchella esculenta* L. by chemical and electrochemical methods at multiwall carbon nanotube paste electrode. *J. Food Meas. Charact.* **2019**, *13*, 1805–1819. [[CrossRef](#)]
192. Djitieu Deutchoua, A.D.; Ngueumaleu, Y.; Dedzo, G.K.; Tonle, I.K.; Ngame, E. Electrochemical study of DPPH incorporated in carbon paste electrode as potential tool for antioxidant properties determination. *Electroanalysis* **2019**, *31*, 335–342. [[CrossRef](#)]
193. Muhammad, H.; Tahiri, I.A.; Qasim, M.; Versiani, M.A.; Hanif, M.; Gul, B.; Ali, S.T.; Ahmed, S. Electrochemical determination of antioxidant activity and HPLC profiling of some dry fruits. *Monatsh. Chem.* **2019**, *150*, 1195–1203. [[CrossRef](#)]
194. Nikolic, M.D.; Pavlovic, A.N.; Mitic, S.S.; Tomic, S.B.; Mitic, M.N.; Kalicanin, B.M.; Manojlovic, D.D.; Stankovic, D.M. Use of cyclic voltammetry to determine the antioxidant capacity of berry fruits: Correlation with spectrophotometric assays. *Eur. J. Hort. Sci.* **2019**, *84*, 152–160. [[CrossRef](#)]

195. Ricci, A.; Teslic, N.; Petropolus, V.-I.; Parpinello, G.P.; Versari, A. Fast analysis of total polyphenol content and antioxidant activity in wines and oenological tannins using a flow injection system with tandem diode array and electrochemical detections. *Food Anal. Methods* **2019**, *12*, 347–354. [[CrossRef](#)]
196. Pilaquinga, F.; Amaguaña, D.; Morey, J.; Moncada-Basualto, M.; Pozo-Martínez, J.; Olea-Azar, C.; Fernández, L.; Espinoza-Montero, P.; Jara-Negrete, E.; Meneses, L.; et al. Synthesis of silver nanoparticles using aqueous leaf extract of *Mimosa albida* (Mimosoideae): Characterization and antioxidant activity. *Materials* **2020**, *13*, 503. [[CrossRef](#)]
197. Aravena-Sanhueza, F.; Pérez-Rivera, M.; Castillo-Felices, R.; Mundaca-Urbe, R.; Aranda Bustos, M.; Peña Farfal, C. Determination of antioxidant capacity (orac) of *Greigia sphacelata* and correlation with voltammetric methods. *J. Chil. Chem. Soc.* **2020**, *65*, 4925–4928. [[CrossRef](#)]
198. Banica, F.; Bungau, S.; Tit, D.M.; Behl, T.; Otrisal, P.; Nechifor, A.C.; Gitea, D.; Pavel, F.-M.; Nemeth, S. Determination of the total polyphenols content and antioxidant activity of *Echinacea Purpurea* extracts using newly manufactured glassy carbon electrodes modified with carbon nanotubes. *Proceses* **2020**, *8*, 833. [[CrossRef](#)]
199. Schilder, W.H.; Tanumihardja, E.; Leferink, A.M.; van den Berg, A.; Olthuis, W. Determining the antioxidant properties of various beverages using staircase voltammetry. *Heliyon* **2020**, *6*, e04210. [[CrossRef](#)]
200. Stevanovic, M.; Stevanovic, S.; Mihailovic, M.; Kiprovski, B.; Bekavac, G.; Mikulic-Petkovsek, M.; Lovic, J. Antioxidant capacity of dark red corn-biochemical properties coupled with electrochemical evaluation. *Rev. Chim.* **2020**, *71*, 31–41. [[CrossRef](#)]
201. Gevaerd, A.; da Silva, B.M.; de Oliveira, P.R.; Marcolino, L.H.; Bergamini, M.F. A carbon fiber ultramicroelectrode as a simple tool to direct antioxidant estimation based on caffeic acid oxidation. *Anal. Methods* **2020**, *12*, 3608–3616. [[CrossRef](#)] [[PubMed](#)]
202. Fu, Y.; You, Z.; Xiao, A.; Liu, L.; Zhou, W. Electrochemical evaluation of the antioxidant capacity of natural compounds on glassy carbon electrode modified with guanine-, polythionine-, and nitrogen-doped graphene. *Open Chem.* **2020**, *18*, 1054–1063. [[CrossRef](#)]
203. Demir, E.; Senocak, A.; Tassembledo-Koubangoye, M.F.; Demirbas, E.; Aboul-Enein, H.Y. Electrochemical evaluation of the total antioxidant capacity of Yam food samples on a polyglycine-glassy carbon modified electrode. *Curr. Anal. Chem.* **2020**, *16*, 176–183. [[CrossRef](#)]
204. Zrinski, I.; Pungjunun, K.; Martinez, S.; Zavagnik, J.; Stankovic, D.; Kalcher, K.; Mehmeti, E. Evaluation of phenolic antioxidant capacity in beverages based on laccase immobilized on screen-printed carbon electrode modified with graphene nanoplatelets and gold nanoparticles. *Microchem. J.* **2020**, *152*, 104282. [[CrossRef](#)]
205. Oualcadi, Y.; Aityoub, A.; Berrekhis, F. Investigation of different antioxidant capacity measurements suitable for bioactive compounds applied to medicinal plants. *J. Food Meas. Charact.* **2021**, *15*, 71–83. [[CrossRef](#)]
206. Pisoschi, A.M.; Pop, A.; Serban, A.I.; Fafaneata, C. Electrochemical methods for ascorbic acid determination. *Electrochim. Acta* **2014**, *121*, 443–460. [[CrossRef](#)]
207. Rueda, M.; Aldaz, A.; Sanchez-Burgos, F. Oxidation of L-ascorbic acid on a gold electrode. *Electrochim. Acta* **1978**, *23*, 419–424. [[CrossRef](#)]
208. Koh, S.N.; Tan, W.T.; Zainal, Z.; Zawawi, R.M.; Zidan, M. Detection of ascorbic acid at glassy carbon electrode modified by single-walled carbon nanotube/zinc oxide. *Int. J. Electrochem. Sci.* **2013**, *8*, 10557–10567.
209. Olana, B.N.; Kitte, S.A.; Soreta, T.R. Electrochemical determination of ascorbic acid at p-phenylenediamine film-holes modified glassy carbon electrodes. *J. Serb. Chem. Soc.* **2015**, *80*, 1161–1175. [[CrossRef](#)]
210. Janeiro, P.; Brett, A.M.O. Catechin electrochemical oxidation mechanisms. *Anal. Chim. Acta* **2004**, *518*, 109–115. [[CrossRef](#)]
211. McCreery, R.L. Advanced carbon electrode materials for molecular electrochemistry. *Chem. Rev.* **2008**, *108*, 2646–2687. [[CrossRef](#)]
212. Rocheleau, M.-J.; Purdy, W.C. The application of quaternary ammonium ionic polymers to electroanalysis: Part 2. Voltammetric studies with quaternary ammonium functionalized polymer film-coated electrodes. *Electroanalysis* **1991**, *3*, 935–939. [[CrossRef](#)]
213. Dalmaso, P.R.; Pedano, M.L.; Rivas, G.A. Electrochemical determination of ascorbic acid and paracetamol in pharmaceutical formulations using a glassy carbon electrode modified with multi-wall carbon nanotubes dispersed in polyhistidine. *Sens. Actuators B Chem.* **2012**, *173*, 732–736. [[CrossRef](#)]
214. Rychagov, A.Y.; Urisson, N.A.; Volkovich, Y.M. Electrochemical characteristics and properties of the surface of activated carbon electrodes in a double-layer capacitor. *Russ. J. Electrochem.* **2001**, *37*, 1172–1179. [[CrossRef](#)]
215. Hassanpour, S.; Behnam, B.; Baradaran, B.; Hashemzadeh, M.; Oroojalian, F.; Mokhtarzadeh, A.; de la Guardia, M. Carbon based nanomaterials for the detection of narrow therapeutic index pharmaceuticals. *Talanta* **2021**, *221*, 121610. [[CrossRef](#)]
216. Yang, C.; Denno, M.E.; Pyakurel, P.; Venton, B.J. Recent trends in carbon nanomaterial-based electrochemical sensors for biomolecules: A review. *Anal. Chim. Acta* **2015**, *887*, 17–37. [[CrossRef](#)] [[PubMed](#)]
217. Jariwala, D.; Sangwan, V.K.; Lauhon, L.J.; Marks, T.J.; Hersam, M.C. Carbon nanomaterials for electronics, optoelectronics, photovoltaics, and sensing. *Chem. Soc. Rev.* **2013**, *42*, 2824–2860. [[CrossRef](#)] [[PubMed](#)]
218. Yang, W.; Ratinac, K.R.; Ringer, S.P.; Thordarson, P.; Gooding, J.J.; Braet, F. Carbon nanomaterials in biosensors: Should you use nanotubes or graphene? *Angew. Chem. Int. Ed.* **2010**, *49*, 2114–2138. [[CrossRef](#)] [[PubMed](#)]
219. Rashidi, A.; Omidi, M.; Choolaei, M.; Nazarzadeh, M.; Yadegari, A.; Haghiosadat, F.; Oroojalian, F.; Azhdari, M. Electromechanical properties of vertically aligned carbon nanotube. In *Advanced Materials Research*; Trans Tech Publ: Stafa-Zurich, Switzerland, 2013; Volume 705, pp. 332–336. [[CrossRef](#)]

220. Eguílaz, M.; Dalmasso, P.R.; Rubianes, M.D.; Gutierrez, F.; Rodríguez, M.C.; Gallay, P.A.; Mujica, M.E.L.; Ramírez, M.L.; Tettamanti, C.S.; Montemerlo, A.E. Recent advances in the development of electrochemical hydrogen peroxide carbon nanotube-based (bio) sensors. *Curr. Opin. Electrochem.* **2019**, *14*, 157–165. [[CrossRef](#)]
221. Scida, K.; Stege, P.W.; Haby, G.; Messina, G.A.; García, C.D. Recent applications of carbon-based nanomaterials in analytical chemistry: Critical review. *Anal. Chim. Acta* **2011**, *691*, 6–17. [[CrossRef](#)] [[PubMed](#)]
222. Huang, S.; Wu, P.F.; Yue, H.Y.; Gao, X.; Song, S.S.; Guo, X.R.; Chen, H.T. ZnO nanosheet arrays/graphene foam: Voltammetric determination of dopamine in the presence of ascorbic acid and uric acid. *J. Mater. Sci. Mater. Electron.* **2019**, *30*, 16510–16517. [[CrossRef](#)]
223. Svancara, I.; Vytras, K.; Barek, J.; Zima, J. Carbon paste electrodes in modern electroanalysis. *Crit. Rev. Anal. Chem.* **2001**, *31*, 311–345. [[CrossRef](#)]
224. Wang, J. *Analytical Electrochemistry*, 2nd ed.; Wiley-VCH: New York, NY, USA, 2000.
225. Ambaye, A.D.; Kefeni, K.K.; Mishra, S.B.; Nxumalo, E.N.; Ntsendwana, B. Recent developments in nanotechnology-based printing electrode systems for electrochemical sensors. *Talanta* **2021**, *225*, 121951. [[CrossRef](#)]